STATE OF CALIFORNIA • DEPARTMENT OF TRANSPORTATION
TECHNICAL REPORT DOCUMENTATION PAGE
TR0003 (REV 10/98)

1. REPORT NUMBER	2. GOVERNMENT ASSOCIATION NUMBER	3. RECIPIENT'S CATALOG NUMBER
CA16-2535		

4. TITLE AND SUBTITLE
Coordination of Freeway Ramp Meters and Arterial Traffic Signals Phase IIA – Site Selection and Simulation Development

5. REPORT DATE
June 2016

6. PERFORMING ORGANIZATION CODE

7. AUTHOR
Alex Skabardonis and Xiao-Yun Lu, California PATH, UC Berkeley

8. PERFORMING ORGANIZATION REPORT NO.
UCB-ITS-PRR-2016-02

9. PERFORMING ORGANIZATION NAME AND ADDRESS
University of California, Berkeley
Institute of Transportation Studies
109 McLaughlin Hall
Berkeley, CA 94720

10. WORK UNIT NUMBER

11. CONTRACT OR GRANT NUMBER
Contract 65A0518

12. SPONSORING AGENCY AND ADDRESS
Division of Research, Innovation and System Information
P.O. Box 942873, MS-83
Sacramento, CA 94273

13. TYPE OF REPORT AND PERIOD COVERED
Final Report, June 1, 2014 - June 30, 2016

14. SPONSORING AGENCY CODE

15. SUPPLEMENTARY NOTES

16. ABSTRACT

The independent operation of freeway ramp meters and the adjacent arterial traffic signals often causes queue spill-back on the freeway on-ramps and the surface street network that result in activation of queue override, which negates the benefits of ramp metering. The objectives of this study are to develop and implement a control algorithm for coordinated operation of metered freeway on-ramps and adjacent signalized intersections. The report describes the research performed in phase IIA of the project: development of a control algorithm, test site selection, and evaluation of a proposed algorithm on the test site through simulation. The field implementation and testing of the proposed algorithm at the selected test site will take place in the upcoming phase IIB of the project.

A control algorithm was developed and evaluated at a real-world test site. The algorithm considers the available on-ramp storage and dynamically reduces the cycle length in order to avoid on-ramp queue spill-back and mitigate unnecessary delay in the conflicting directions. The simulation results show the proposed coordination strategy eliminated the queue spill-back on the metered on-ramps that activate the queue override. This resulted in 17.9% reduction on freeway delay. The analysis of field data on bottleneck discharge flows indicate that the proposed strategy may improve the freeway capacity by 5 to 10 percent. The delay on the parallel arterial was increased on the approaches feeding the on-ramps but decreased on the rest of the signal controlled approaches. The system-wide delay was reduced by 7 percent.

17. KEY WORDS
Freeway ramp metering (RM), Integrated corridor management (ICM), Coordination of Freeway Ramp Meters (CRM)

18. DISTRIBUTION STATEMENT
No restrictions. This document is available to the public through the National Technical Information Service, Springfield, VA 22161

19. SECURITY CLASSIFICATION *(of this report)*

20. NUMBER OF PAGES
72

21. COST OF REPORT CHARGED

Reproduction of completed page authorized.

DISCLAIMER STATEMENT

Coordination of Freeway Ramp Meters and Arterial Traffic Signals Phase IIA – Site Selection and Simulation Development

David Ken
Xiao-Yun Lu
Alexander Skabardonis

The contents of this report reflect the views of the authors who are responsible for the facts and accuracy of the data presented herein. The contents do not necessarily reflect the official views or policies of the State of California. This publication does not constitute a standard, specification or regulation.

June 2016

CALIFORNIA PARTNERS FOR ADVANCED TRANSIT AND HIGHWAYS

ABSTRACT

The independent operation of freeway ramp meters and the adjacent arterial traffic signals often causes queue spillback on the freeway on-ramps and the surface street network that result in activation of queue override, which negates the benefits of ramp metering. The objectives of this study are to develop and implement a control algorithm for coordinated operation of metered freeway on-ramps and adjacent signalized intersections. The report describes the research performed in phase IIA of the project: development of a control algorithm, test site selection, and evaluation of a proposed algorithm on the test site through simulation. The field implementation and testing of the proposed algorithm at the selected test site will take place in the upcoming phase IIB of the project.

A control algorithm was developed and evaluated at a real-world test site. The algorithm considers the available on-ramp storage and dynamically reduces the cycle length in order to avoid on-ramp queue spillback and mitigate unnecessary delay in the conflicting directions. The simulation results show the proposed coordination strategy eliminated the queue spillback on the metered on-ramps that activate the queue override. This resulted in 17.9% reduction on freeway delay. The analysis of field data on bottleneck discharge flows indicate that the proposed strategy may improve the freeway capacity by 5 to 10 percent. The delay on the parallel arterial was increased on the approaches feeding the on-ramps but decreased on the rest of the signal controlled approaches. The system-wide delay was reduced by 7 percent.

ACKNOWLEDGEMENTS

EXECUTIVE SUMMARY

Objectives and Methodology

Integrated corridor management (ICM) of highway facilities comprised of freeways and adjacent arterial streets offers considerable potential in managing traffic congestion and reducing adverse environmental impacts. However, currently freeway control systems (mostly on-ramp ramp metering) and the traffic signals on adjacent arterial facilitating freeway access operate independently under day-to-day recurrent conditions.

The objectives of the research project described in this report are to develop and implement a control algorithm to manage the entry of vehicles on the on-ramp through signal timing changes at the intersections along adjacent arterial(s). The research effort is a continuation of a previous PATH research project that developed a control algorithm for coordinating a single freeway metered on-ramp with an adjacent isolated signalized intersection. This report describes the research performed in phase IIA of the project: development of a control algorithm, test site selection, and evaluation of a proposed algorithm on the test site through simulation. The field implementation and testing of the proposed algorithm at the selected test site will take place in the upcoming phase IIB of the project.

- **Literature Review:** Existing studies have focused on diversion strategies for freeway traffic to arterials under incident conditions. Control strategies proposed to manage arterial traffic to prevent overflow on freeway on-ramps have shortcomings. Furthermore there is a lack of field implementation and evaluation of freeway arterial coordination strategies.

- **Test Site Selection:** The selected site is a three mile section of northbound I-680 from Alum Rock Ave. to Berryless Rd. and a section of Capitol Ave. arterial with 5 signalized intersections in the city of San Jose. The site selection was based on several criteria including I) presence of active bottlenecks in the test section, ii) free-flow conditions at the study section boundaries, ii) functional loop detector system, iv) size: the freeway segment should be up to 5 miles, and the parallel arterial should have no more than 5 major signalized intersections and v) cooperation among jurisdictions managing the system. The test site was simulated with the AIMSUN microscopic simulation model. The model was calibrated against field data to reasonably replicate observed traffic conditions.

- **Development of Control Strategies:** Three control strategies have been developed to manage the entry of arterial traffic on the freeway on-ramp to avoid queue spillover. The first algorithm is an extension of the algorithm originally developed in the previous PATH project and adjusts both the metering rates and signal settings. The second algorithm adjusts the arterial signal settings taking into account the platoons on the arterial. The third algorithm attempts to minimize the on-ramp queues through changes of the cycle length at the adjacent signals. The third algorithm (queue length minimization) was selected for evaluation through simulation at the test site.

- **Empirical Study:** A field study has been conducted at one of the active bottlenecks at the selected site to field measure the changes in freeway discharge rate (capacity) due to the activation of queue override. Data were collected over ten weekdays using video cameras. Traffic flows on the freeway mainline and on-ramp were recorded an analyzed for the 7:00-9:30 AM peak period.

Summary of the Findings and Recommendations

The simulation results show the proposed coordination strategy eliminated the queue spillback on the metered on-ramps that activate the queue override. This resulted in 17.9% reduction on freeway delay. The analysis of field data on bottleneck discharge flows indicate that the proposed strategy may improve the freeway capacity by 5 to 10 percent. The delay on the parallel arterial was increased on the approaches feeding the on-ramps but decreased on the rest of the signal controlled approaches. The system-wide delay was reduced by 7 percent.

The proposed control algorithm can be used with any freeway on-ramp metering algorithm. The proposed algorithm is simple and readily implementable at most freeway corridors with metered on-ramps and adjacent signalized arterials without additional instrumentation.

The next step in the ongoing research is conducting the Phase IIB of the project: field implementation and testing of the control algorithm at the selected test site. This phase of the project involves the following major tasks: a) strategy software implementation and testing, b) field implementation, c) data collection on traffic performance on both freeway and arterial intersections, and d) analysis of field data to assess algorithm performance and develop guidelines for statewide implementation.

TABLE OF CONTENTS

LIST OF FIGURES

LIST OF TABLES

CHAPTER 1

INTRODUCTION

1.1 Problem Statement

Integrated corridor management (ICM) of highway facilities comprised of freeways and adjacent arterial streets offers considerable potential in managing traffic congestion and reducing adverse environmental impacts. However, currently freeway control systems (mostly on-ramp ramp metering) and the traffic signals on adjacent arterial facilitating freeway access operate independently under day-to-day recurrent conditions.

During peak hours, freeway ramp metering restricts the flow of on-ramp traffic entering the freeway mainline in order to reduce the conflict between on-ramp and mainline traffic. Such approach mitigates or prevents capacity drop at locations with high on-ramp demand, and therefore maximizes the capacity of the freeway (mainline and on-ramp). However, under independent operation, the arterial traffic signals facilitating freeway access fail to recognize that the metered on-ramps are oversaturated due to reduced capacity and limited storage space. Instead, the arterial traffic signals respond to the peak hour demand by providing long cycles therefore long green durations and progressively coordinating traffic signals along the major arterial that channels traffic entering the freeway, in order to maximize arterial capacity. This may lead to platoons of arterial traffic advancing to the oversaturated on-ramps and thus excessive queues on the on-ramps, which can cause spillback on the adjacent arterial. The queue spillback will not only impede the conflicting directions of the arterial traffic, it will also necessitate queue override at the metered on-ramps, which releases the on-ramp queue onto the freeway and reduces its capacity.

1.2 Project Objectives

The objectives of the research project described in this report are to develop and implement a control algorithm to manage the entry of vehicles on the on-ramp through signal timing changes at the intersections along adjacent arterial(s). The proposed algorithm is an extension of a control algorithm that was originally developed in a previous PATH for coordinating a single freeway metered on-ramp with an adjacent isolated signalized intersection [12]. The report describes the research performed in phase IIA of the project: development of a control algorithm, test site selection, and evaluation of a proposed algorithm on the test site through simulation. The field implementation and testing of the proposed algorithm at the selected test site will take place in the upcoming phase IIB of the project.

1.3 Report Organization

Chapter 2 provides an overview of recent research in the area of coordinating freeway ramp metering and arterial traffic signals. Chapter 3 describes the test site selection process, and presents the characteristics of the selected site. Chapter 4 describes the three control strategies developed and the recommended control strategy to be tested in simulation and the field. Chapter 5 details the microscopic simulation model, its calibrated procedures, and the results of the simulations tests. Chapter 6 presents the results from a field study on the effect of queue override on the freeway discharge rate, performed to supplement the simulation results. The final chapter 7 summarizes the study findings and recommends the appropriate control strategy to be tested in the upcoming field implementation.

CHAPTER 2

LITERATURE REVIEW

Existing research has focused on development of optimization algorithms and routing models for integrated control of freeway-arterial corridor system with emphasis on non-recurrent (incident related) congestion. Other approaches focus on control strategies for freeway interchanges to avoid off-ramp queue spillback, and algorithms that prevent overflow on metered ramps that adversely affect arterial operations under recurrent congestion. Representative approaches are presented in the next three sections.

2.1 Freeway Traffic Diversion

There are several studies on diverting freeway traffic onto adjacent arterials, mostly in non-recurrent conditions such as incidents on freeways. Such scenarios typically involve how to effectively utilize the spare capacity of the adjacent arterials in the event of temporary freeway capacity reduction, in order to prevent major freeway breakdown. They do not address how to efficiently coordinate metered on-ramps and adjacent arterials.

Recently, the Federal Highway Administration released a manual for coordinated freeway and arterial operation [1] but the document does not provide any control strategies for coordinated operation of freeway and arterial. This document outlined the practical issues such as institutional barriers, technological challenges, and integration of intelligent transportation systems. The manual also provided examples of freeway-arterial corridors that have implemented coordinated operation schemes, however, these examples only show how local arterials can be coordinated with the freeway in the event of an incident and help divert some freeway traffic by utilizing the excess capacity on the local arterials.

Control strategies for traffic diversion adjust ramp metering rates and arterial traffic signal timing plans in order to facilitate high volumes of freeway traffic exit the freeway, travel on the adjacent parallel arterial efficiently, and quickly return to the freeway immediately downstream of a capacity-constrained location such as an area with incidents. Tian et al [2] proposed a traffic-responsive coordination strategy that extends the green times corresponding to the freeway off-ramps and parallel arterial and maximizes ramp meter rates of the downstream on-ramps based on real time queue detection on the freeway, and it was shown to be effective for freeway-arterial corridors with consecutive diamond interchanges. In addition, the work by Zhang et al [3] tested a similar approach at a corridor with various configurations of freeway interchanges. Other works in this area include an optimization-based coordination strategy that minimizes corridor level delay during incident diversion [4], an empirical study of the effect of dynamic traveler information on the amount of freeway traffic diverted and the corridor-wide performance [5], and a control strategy for diverting traffic from the freeway to the adjacent arterials with significant spare capacity, in the event of periodic freeway capacity reduction [6].

2.2 Off-ramp Bottleneck

Several studies investigated the queue spillback of off-ramp freeway traffic onto the freeway mainline. Off-ramp bottlenecks typically are created because of inefficient signal timing at the downstream end of the freeway off-ramp, when it intersects the adjacent arterial. Recently Yang et al [7] proposed conditional signal priority for off-ramp traffic in order to mitigate the impact of off-ramp spillback on freeway performance, and this was enhanced in [8] by incorporating downstream arterial signal progression to quickly discharge the off-ramp queue and further reduce the impact of off-ramp spillback.

2.3 Coordination of Freeway On-ramp and Adjacent Arterial

Few studies have addressed the inefficient control of freeway ramp metering and the nearby arterial corridor facilitating freeway access in the day-to-day recurrent conditions, and no generalizable control strategies have been implemented.

Tian et al [9] developed an algorithm for diamond interchanges that reduces green durations for movements with on-ramp access to prevent on-ramp queue spillback, under the same cycle length. This approach may cause spillback of on-ramp demand onto the upstream arterial, especially under long cycle lengths, and temporary activation of queue override.

Recker et al [10] developed a system-wide optimization model for ramp metering and traffic signals from stochastic queuing theory, but the improvement observed after implementing the control strategy at a network of freeways and arterials was a result of using a more efficient ramp metering control, rather than coordination of ramp metering and traffic signals. Moreover, the proposed approach requires solving non-linear optimization in real time, which is computationally intensive and not feasible in most situations.

Other research efforts focused only on control of isolated signalized intersections at or adjacent to freeway on-ramps. For example, Li and Tao [11] proposed a signal optimization model for an arterial at an isolated freeway interchange using the cell transmission model but neglected ramp metering in their algorithm.

In a recently completed PATH project (Coordination of Freeway Ramp Meters and Arterial Traffic Signals Phase I [12] a signal optimization model was developed that takes the ramp meter rate and on-ramp queue length into account, for an isolated diamond interchange. A brief field test was conducted to show that coordination of freeway ramp metering and arterial traffic signals is technologically feasible and implementable in the real world. However, similar to the method by Tian et al [9], the proposed algorithm simply reallocated green times without changing the cycle length, therefore it provided unnecessarily long green durations for the conflicting movements and disregarded the potential queue spillback into the upstream arterial intersection. Furthermore, the impact of queue override was not considered.

2.4 Summary of Literature Review

Existing studies have focused on diversion strategies for freeway traffic to arterials under incident conditions. Control strategies proposed to manage arterial traffic to prevent overflow on freeway on-ramps have shortcomings. Furthermore there is a lack of field implementation and evaluation of freeway arterial coordination strategies.

CHAPTER 3

TEST SITE SELECTION

This chapter describes the process of test site selection and the characteristics of the site selected for testing the control strategies for coordination of freeway on-ramp metering and arterial signal control. The selected site should be representative of typical freeway corridor segments (4 to 6 mile long) with at least one adjacent arterial facilitating freeway access. The selected corridor should satisfy the following criteria:

3.1 Site Selection Criteria

(1) The freeway corridor should have 3 to 5 freeway-arterial interchanges;

(2) The freeway corridor must not contain any freeway-freeway interchanges;

(3) At least one recurrent bottleneck must be observed during either the morning or the evening peak hours, preferable in only one direction of the freeway;

(4) The recurrent bottleneck(s) must be caused by the high on-ramp demand;

(5) Under recurrent conditions, the bottlenecks observed along the freeway corridor must be isolated (free-flow conditions at the upstream and downstream ends of the corridor);

(6) The physical capacity of a section is fixed except for lane reduction caused by lane closure due to incident/accident;

(7) The freeway corridor must have low frequency of incidents that contribute to non-recurrent delay;

(8) The length of the freeway on-ramps should not be too short or too long (ideally, they should accommodate 30 to 50 queued vehicles);

(9) The corridor must contain at least one parallel arterial adjacent to the freeway;

(10) The parallel arterial(s) must connect the arterials that have interchanges with and are perpendicular to the freeway;

(11) The parallel and perpendicular arterials adjacent to the freeway should be primarily used to facilitate freeway access;

(12) High demand from arterial to freeway should be the main cause of arterial congestion;

(13) No more than 5 major signalized intersections along the parallel arterial;

(14) There should not be high concentration of pedestrians crossing the arterial or bicyclists impeding the arterial traffic flow;

(15) No active work zones on the freeway and the arterial;

(16) Satisfactory detector health and properly functioning ramp meters and traffic signals;

(17) Cooperation between the jurisdictions responsible for the operation and maintenance of the freeway ramp metering and arterial traffic signals control systems;

(18) The selected site must be supported by centralized data acquisition and control system in order to coordinate freeway ramp-metering and arterial traffic signals for field implementation

(19) The selected site must be representative of freeway corridors with adjacent arterial(s) facilitating freeway access.

3.2 Candidate Sites

Six candidate test sites were identified based on extensive data analysis and input from Caltrans and the project panel. The maps of the candidate sites are shown in Figure 3.1 through 3.6. Tables 3.1 through 3.6 detail whether the site selection criteria were satisfied. Unsatisfied criteria are highlighted in red.

3.2.1 Candidate Site #1: I-80 Northbound PM Peak

Segment of interest: Central Ave. to Pinole Valley Rd (9 miles)

Parallel arterial: San Pablo Ave (15 major signalized intersections)
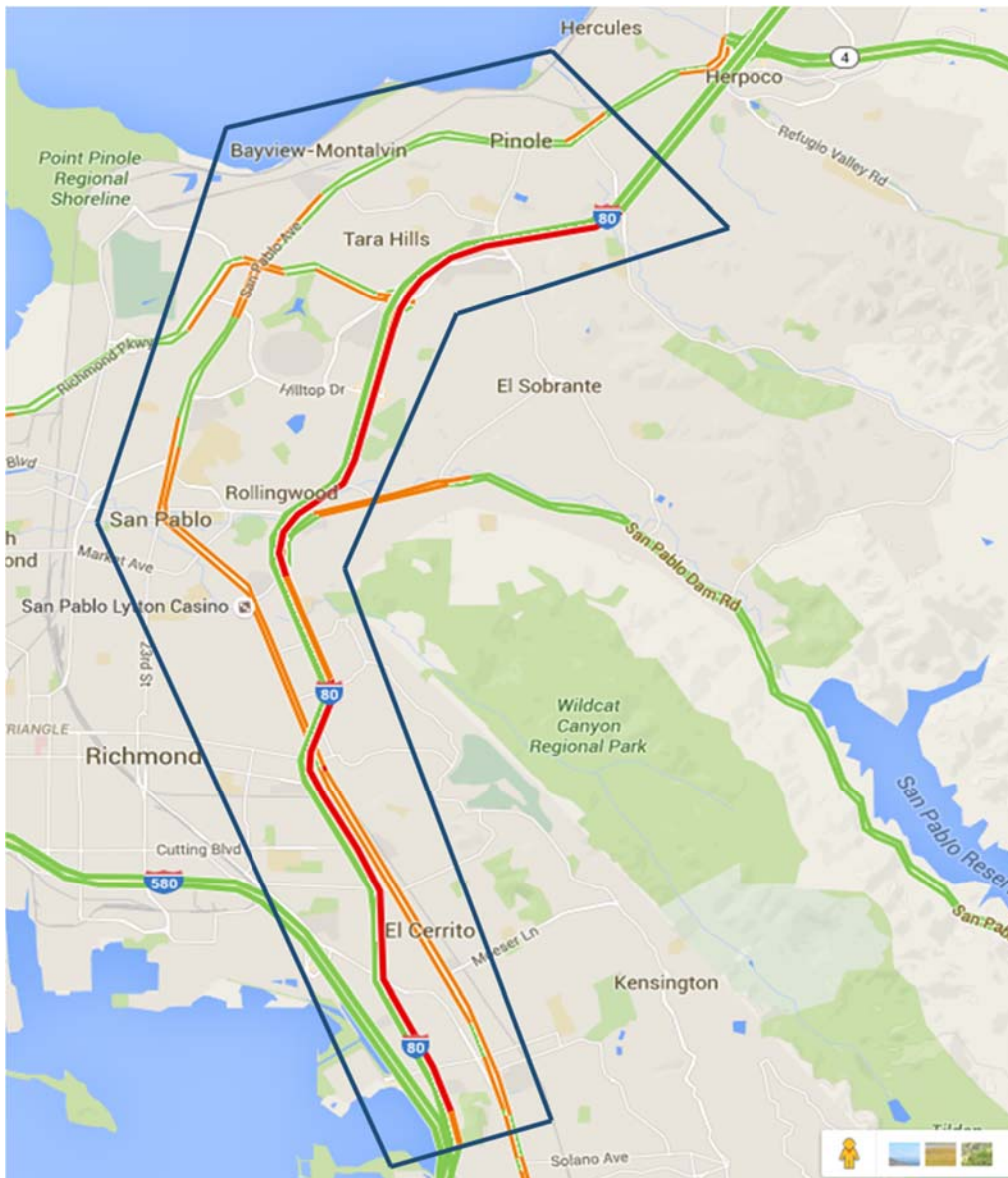
Figure 3.1 Map of I-80 Northbound PM Peak and San Pablo Ave

Table 3.1 Comments for Candidate Site #1: I-80 Northbound PM Peak and San Pablo Ave

Criteria	Comments
(1)	There are 10 freeway-arterial interchanges.
(2)	No freeway-to-freeway interchange.
(3)	Multiple recurrent bottlenecks.
(4)	Recurrent congestion is mostly caused by high on-ramp demand but also high off-ramp demand at a few locations (i.e. San Pablo Dam Rd.).
(5)	Free-flow conditions can be observed upstream of Central Ave. (up to the I-580 split) and downstream of Pinole Valley Rd.
(6)	The freeway capacity is fixed.
(7)	There is relatively high frequency of incidents/accidents that contribute to significant non-recurrent delay.
(8)	The on-ramp lengths fit the requirement with the exception of San Pablo Dam Rd. and Solano Ave. on-ramps.
(9)	San Pablo Ave. is a major arterial near the freeway.
(10)	San Pablo Ave. connects the perpendicular arterials with freeway access but the road geometry is less than ideal because San Pablo Ave is too far from I-80 downstream of San Pablo Dam Rd.
(11)	San Pablo Ave. is not primarily used to facilitate freeway access.
(12)	High demand for freeway access is not the main cause of oversaturation on San Pablo Ave.
(13)	There are roughly 15 major signalized intersections along San Pablo Ave.
(14)	There is limited pedestrian and bicyclist traffic due to the suburban setting.
(15)	There were no active work zones at the time of site selection but the schedule of future construction activities on the corridor conflict with the timelines for field data collection and implementation.
(16)	Very good detector health (almost 100% observed), and the traffic signals are properly functioning.
(17)	Cooperation among different jurisdictions is uncertain. Multiple agencies (i.e. City of El Cerrito, City of Richmond, City of San Pablo, etc.) must be involved, in addition to Caltrans.
(18)	Multiple agencies operate the arterial traffic signal, thus it is very difficult to have the site supported by centralized data system and control system.
(19)	The unique road geometry makes the site less representative of typical freeway-arterial corridors.

3.2.2 Candidate Site #2: I-680 Northbound AM Peak

Segment of interest: Capitol Expy. To Berryessa Rd (4 miles)

Parallel arterial: Capitol Ave (5 major signalized intersections)
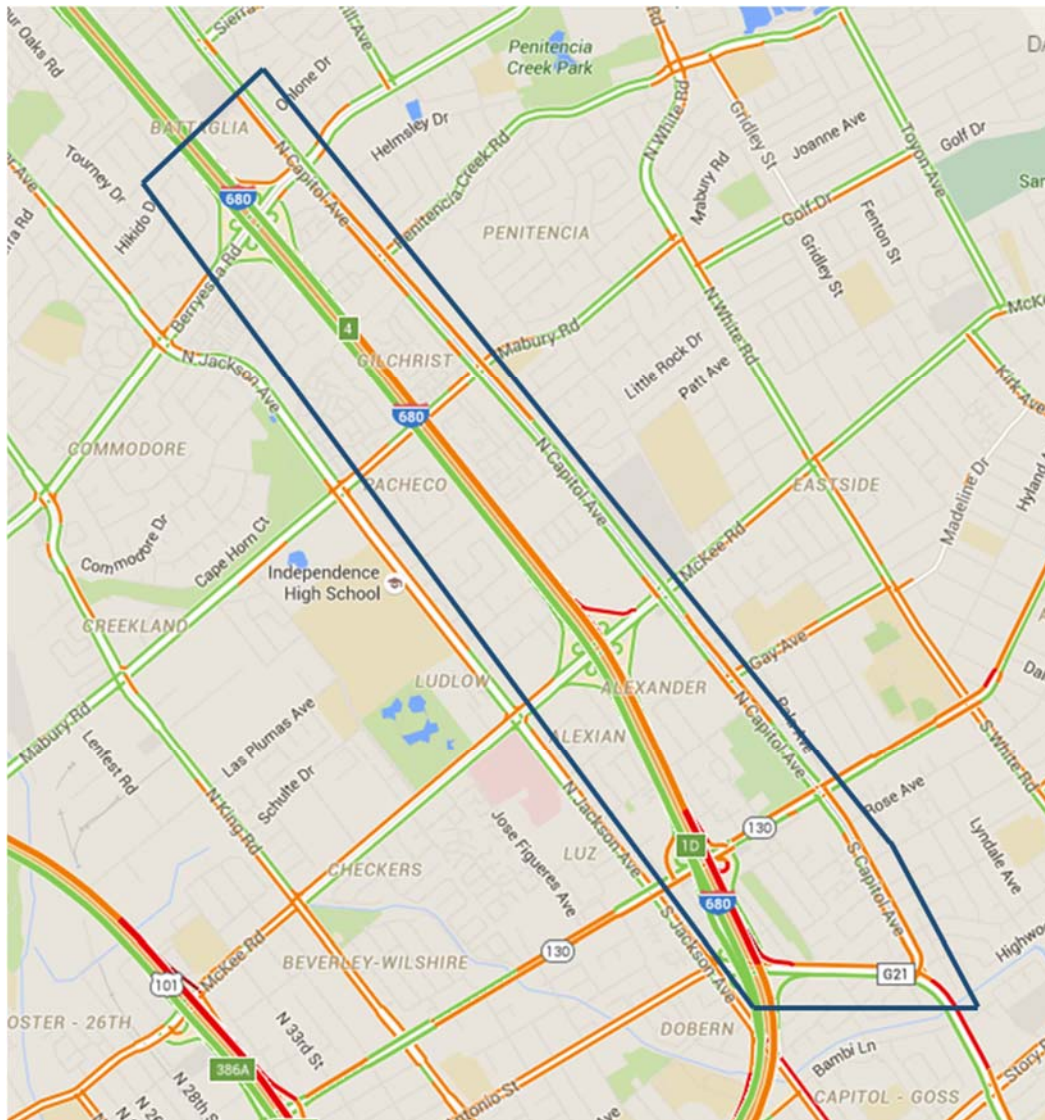
Figure 3.2 Map of I-680 Northbound AM Peak and Capitol Ave

Table 3.2 Comments for Candidate Site #2: I-680 Northbound AM Peak and Capitol Ave

Criteria	Comments
(1)	There are 4 freeway-arterial interchanges.
(2)	No freeway-to-freeway interchange.
(3)	Multiple recurrent bottlenecks.
(4)	Recurrent congestion is primarily caused by high on-ramp demand.
(5)	Free-flow conditions can be observed upstream of Capitol Expy., and downstream of Berryessa Rd.
(6)	The freeway capacity is fixed.
(7)	Very low frequency of incidents and non-recurrent delay.
(8)	The on-ramp lengths fit the requirement. There is sufficient storage on all on-ramps.
(9)	Capitol Ave. is a major arterial immediately adjacent to the freeway.
(10)	Capitol Ave. connects the perpendicular arterials with freeway access and the road geometry resemble that of a grid network.
(11)	Capitol Ave. is primarily used to facilitate freeway access during the morning peak.
(12)	High demand for freeway access is the main cause of oversaturation on the arterials.
(13)	There are 5 major signalized intersections along Capitol Ave.
(14)	There is limited pedestrian and bicyclist traffic due to the suburban setting.
(15)	There were no active work zones at the time of site selection. Construction activities for the bus rapid transit project on Alum Rock Ave. (perpendicular arterial) were scheduled to take place after field data collection and will complete before field implementation.
(16)	Good detector health due to newly installed detectors, and the traffic signals are properly functioning.
(17)	Agreement with the City of San Jose has been reached. Santa Clara County has to be involved but it operates only one signalized intersection (Capitol Ave. at Capitol Expy.).
(18)	Under the current agreement between City of San Jose and Caltrans, the site is supported by centralized data system and control system. However, cooperation with Santa Clara County is uncertain.
(19)	The road geometry resembles the typical freeway-arterial corridors.

3.2.3 Candidate Site #3: I-680 Northbound AM Peak

Segment of interest: E. San Antonio St./Capitol Expy to Berryessa Rd (4 miles)

Parallel arterial: Jackson Ave (5 major signalized intersections)
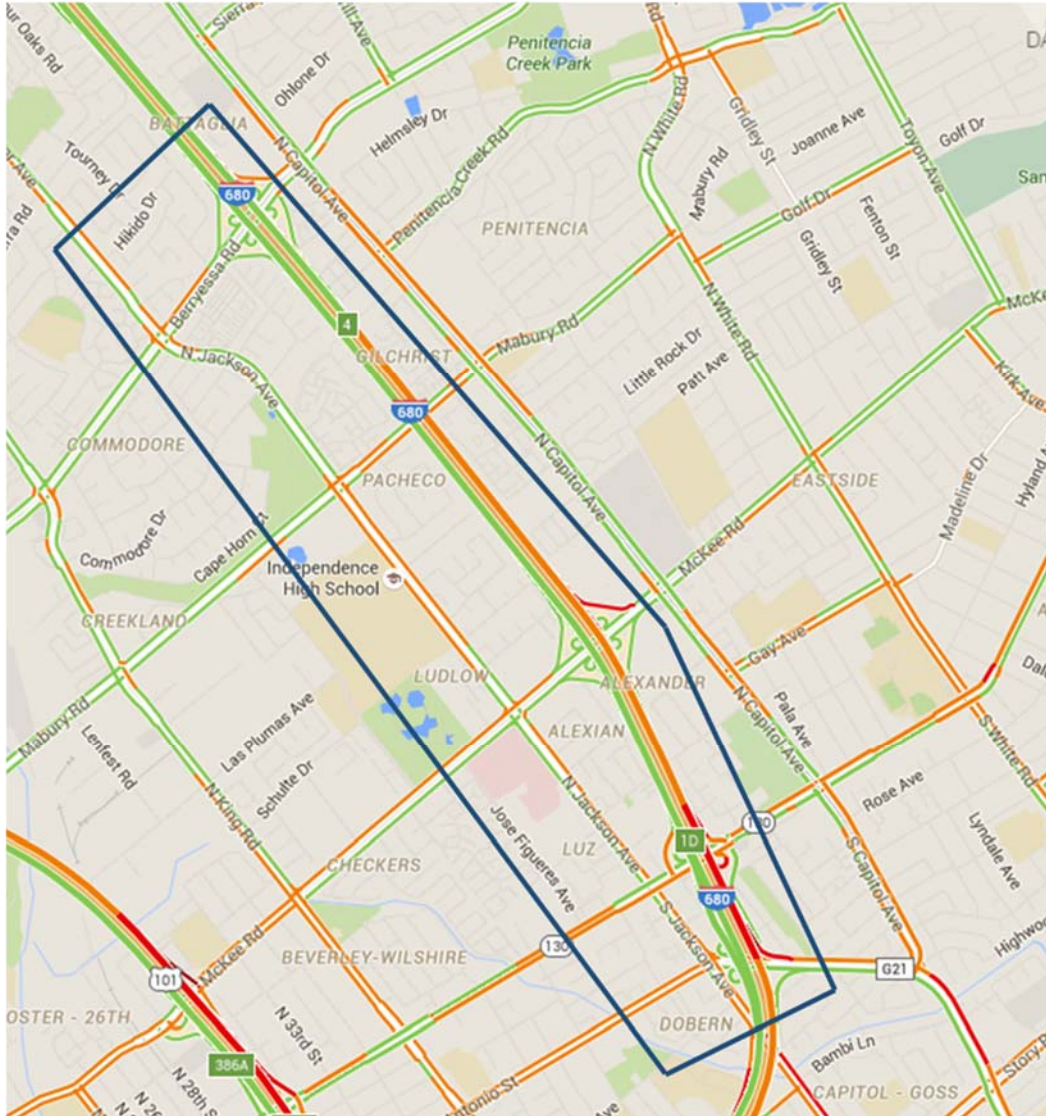
Figure 3.3 Map of I-680 Northbound AM Peak and Jackson Ave

Table 3.3 Comments for Candidate Site #3: I-680 Northbound AM Peak and Jackson Ave

Criteria	Comments
(1)	There are 4 freeway-arterial interchanges.
(2)	No freeway-to-freeway interchange.
(3)	Multiple recurrent bottlenecks.
(4)	Recurrent congestion is primarily caused by high on-ramp demand.
(5)	Free-flow conditions can be observed upstream of Capitol Expy., and downstream of Berryessa Rd.
(6)	The freeway capacity is fixed.
(7)	Very low frequency of incidents and non-recurrent delay.
(8)	The on-ramp lengths fit the requirement. There is sufficient storage on all on-ramps.
(9)	Jackson Ave. is a major arterial immediately adjacent to the freeway.
(10)	Jackson Ave. connects the perpendicular arterials with freeway access and the road geometry resembles that of a grid network.
(11)	Jackson Ave. is used to facilitate freeway access during the morning peak but this is not the arterial's primary function.
(12)	The demand for freeway access is not very high and the parallel arterial is not very saturated.
(13)	There are 5 major signalized intersections along Jackson Ave.
(14)	There is a fair amount of pedestrian traffic due to the presence of schools and hospitals nearby.
(15)	There were no active work zones at the time of site selection. Construction activities for the bus rapid transit project on Alum Rock Ave. (perpendicular arterial) were scheduled to take place after field data collection and will complete before field implementation.
(16)	Good detector health due to newly installed detectors, and the traffic signals are properly functioning.
(17)	Agreement with the City of San Jose have been reached. All of the signalized intersections are operated by the City of San Jose.
(18)	Under the current agreement between City of San Jose and Caltrans, the site is supported by centralized data system and control system.
(19)	The road geometry resembles the typical freeway-arterial corridors.

3.2.4 Candidate Site #4: SR-87 Northbound AM Peak

Segment of interest: Branham Ln. to W. Alma Ave (4 miles)

Parallel arterial: Almaden Expy (5 major signalized intersections)
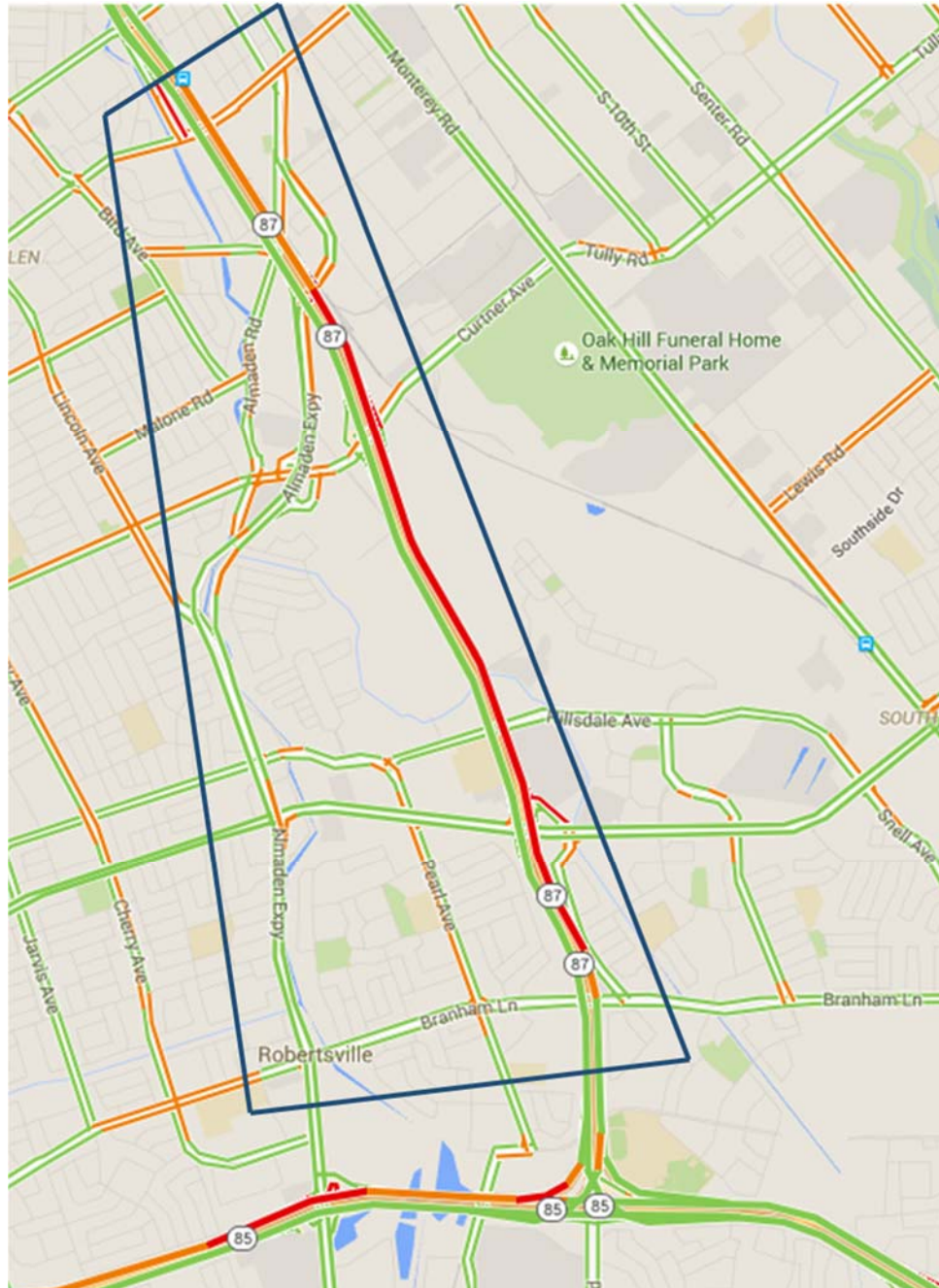
Figure 3.4 Map of SR-87 Northbound AM Peak and Almaden Expy

Table 3.4 Comments for Candidate Site #4: SR-87 Northbound AM Peak and Almaden Expy

Criteria	Comments
(1)	There are 4 freeway-arterial interchanges.
(2)	No freeway-to-freeway interchange.
(3)	Multiple recurrent bottlenecks.
(4)	Recurrent congestion is primarily caused by high on-ramp demand.
(5)	Free-flow conditions can be observed upstream of Capitol Expy., and downstream of Alma Ave.
(6)	The freeway capacity is fixed.
(7)	Very low frequency of incidents and non-recurrent delay.
(8)	The on-ramp lengths fit the requirement. There is sufficient storage on all on-ramps.
(9)	Almaden Expy. is the major arterial near the freeway but not very close to the freeway.
(10)	Almaden Expy. connects the perpendicular arterials with freeway access but the road geometry does not resemble a grid network. In addition, Almaden Expy. has grade separated interchanges rather than signalized intersections with a few of its perpendicular arterials.
(11)	Almaden Expy. is used to facilitate freeway access during the morning peak but this is not the arterial's primary function. Almaden Expy. is often used as an alternate route to SR-87.
(12)	The demand for freeway access is very high and it is the primary cause of arterial congestion.
(13)	There are 5 major signalized intersections along Almaden Expy. but there are also two grade-separated interchanges with the perpendicular arterials.
(14)	Very low pedestrian traffic due to the suburban setting.
(15)	There were no active work zones at the time of site selection. No construction planned for the duration of this project.
(16)	There is extensive coverage of detectors but not all of them are properly functioning. Those at the most important locations are in good condition. The traffic signals are working properly.
(17)	All of the signals on Almaden Expy. are operated by Santa Clara County. Cooperation from this agency is uncertain.
(18)	Under the current agreement between City of San Jose and Caltrans, the site is supported by centralized data system and control system. However, cooperation from Santa Clara County is also required but is uncertain and challenging to obtain.
(19)	The road geometry does not resemble the typical freeway-arterial corridors.

3.2.5 Candidate Site #5: US-101 Northbound AM Peak & PM Peak

Segment of interest: Wilfred Ave. to Baker Ave (4 miles)

Parallel arterial: Santa Rosa Ave (5 major signalized intersections)
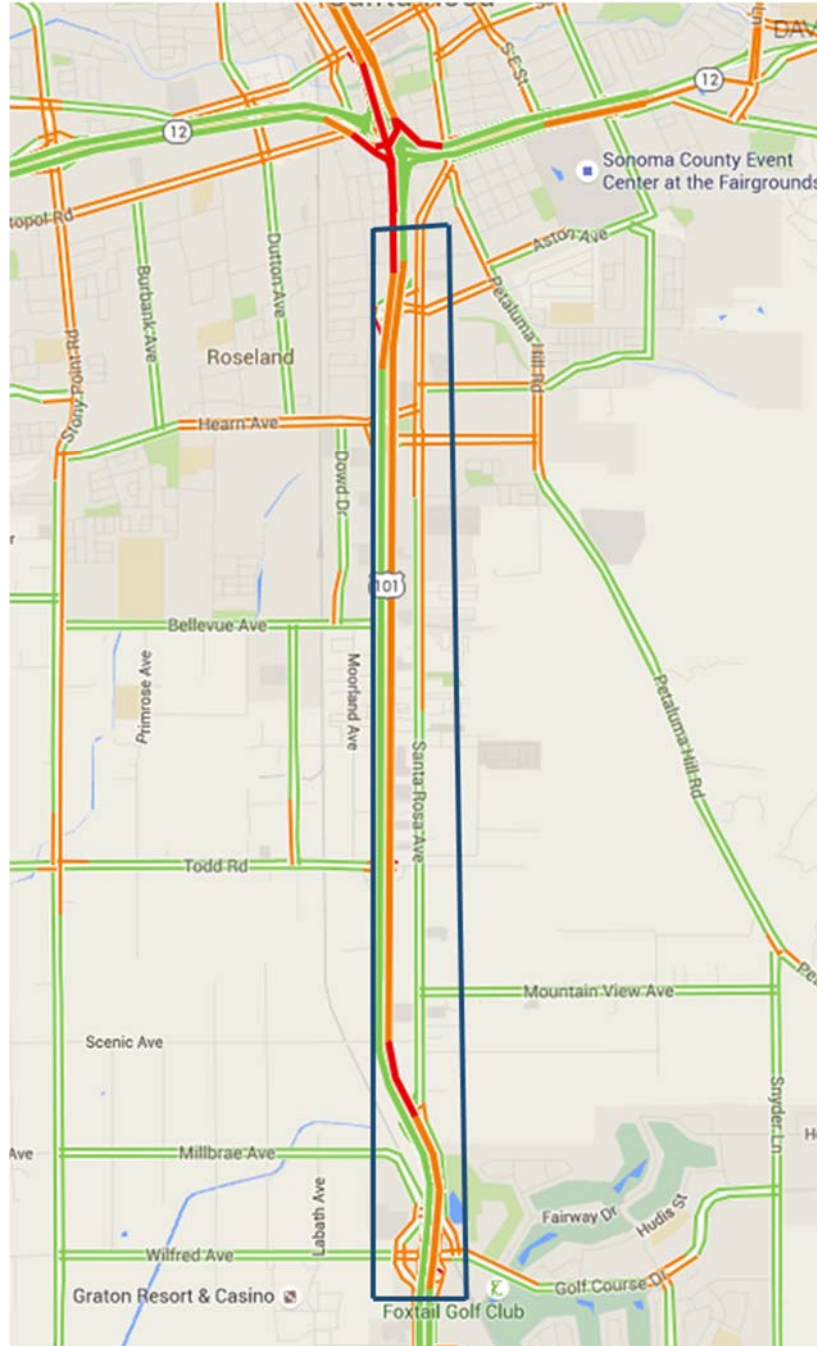
Figure 3.5 Map of US-101 Northbound AM/PM Peak and Santa Rosa Ave

Table 3.5 Comments for Candidate Site #5: US-101 Northbound AM/PM Peak and Santa Rosa Ave

Criteria	Comments
(1)	There are 5 freeway-arterial interchanges.
(2)	No freeway-to-freeway interchange.
(3)	Multiple recurrent bottlenecks.
(4)	Recurrent congestion is primarily caused by high on-ramp demand.
(5)	Free-flow conditions can be observed upstream of Wilfred Ave., and downstream of Baker Ave.
(6)	The freeway capacity is fixed.
(7)	Relatively low frequency of incidents and non-recurrent delay.
(8)	The on-ramp lengths fit the requirement. There is sufficient storage on all on-ramps.
(9)	Santa Rosa Ave. is the major arterial immediately adjacent to the freeway.
(10)	Santa Rosa Ave. connects the perpendicular arterials with freeway access and the road geometry somewhat resembles a grid network.
(11)	Santa Rosa Ave. is used to facilitate freeway access during the peak hours but it is also used as an alternate route to US 101 for shorter trips, mostly due to the rural setting (in areas further away from Santa Rosa) and relatively high speed limit.
(12)	The demand for freeway access is very high and it is the primary cause of arterial congestion.
(13)	There are 5 major signalized intersections along Santa Rosa Ave.
(14)	Very low pedestrian traffic due to the suburban setting.
(15)	There were no active work zones at the time of site selection. No construction planned for the duration of this project.
(16)	There is extensive coverage of detectors and video cameras on the freeway. The traffic signals are working properly.
(17)	Some signals are operated by the City of Santa Rosa while others are operated by the City of Rohnert Park. Cooperation from these agencies is uncertain.
(18)	Due to the uncertainty of whether the City of Santa Rosa and the City of Rohnert Park are willing to participate, whether the site will be supported by centralized data system and control system is unknown.
(19)	The road geometry somewhat resembles the typical freeway-arterial corridors. However, the perpendicular arterials do not connect opposite sides of the freeway.

3.2.6 Candidate Site #6: SR-4 Westbound AM Peak

Segment of interest: Railroad Ave. to Willow Pass Rd (6 miles)

Parallel arterial: Leland Rd (5 major signalized intersections)
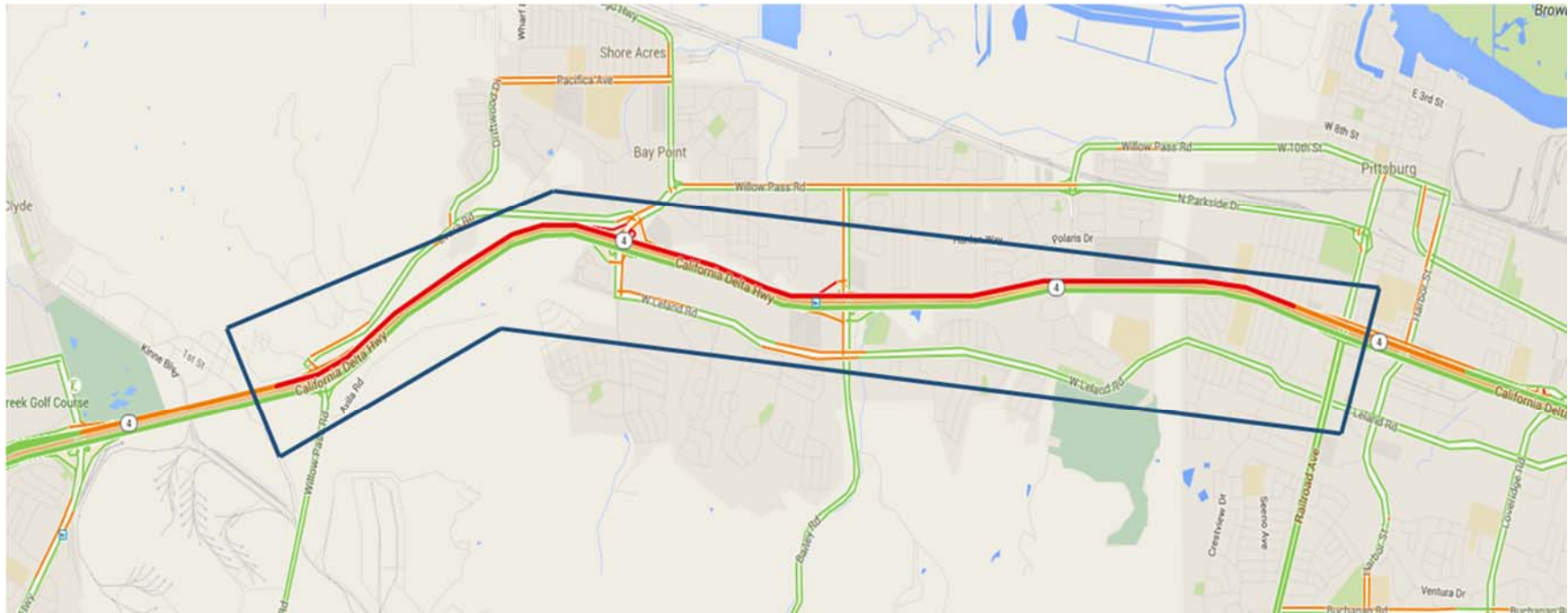
Figure 3.6 Map of SR-4 Westbound AM Peak and Leland Rd

Table 3.6 Comments for Candidate Site #6: SR-4 Westbound AM Peak and Leland Rd

Criteria	Comments
(1)	There are 5 freeway-arterial interchanges.
(2)	No freeway-to-freeway interchange.
(3)	Multiple recurrent bottlenecks.
(4)	Recurrent congestion is primarily caused by high on-ramp demand.
(5)	Free-flow conditions can be observed upstream of Railroad Ave., and downstream of Willow Pass Rd.
(6)	The freeway capacity is fixed.
(7)	Relatively low frequency of incidents and non-recurrent delay.
(8)	The on-ramp lengths fit the requirement. There is sufficient storage on all on-ramps.
(9)	Leland Rd. is the major arterial immediately adjacent to the freeway.
(10)	Leland Rd. connects the perpendicular arterials with freeway access and the road geometry somewhat resembles a grid network.
(11)	Leland Rd. is used to facilitate freeway access during the morning peak hours.
(12)	The demand for freeway access is very high and it is the primary cause of arterial congestion.
(13)	There are 5 major signalized intersections along Leland Rd.
(14)	Very low pedestrian traffic due to the suburban setting.
(15)	There were no active work zones at the time of site selection. No construction planned for the duration of this project.
(16)	The detector health is satisfactory. The traffic signals are working properly.
(17)	Some signals are operated by the City of Bay Point while others are operated by the City of Pittsburg. Cooperation from these agencies is uncertain.
(18)	Due to the uncertainty of whether the City of Bay Point and the City of Pittsburg are willing to participate, whether the site will be supported by centralized data system and control system is unknown.
(19)	The road geometry somewhat resembles the typical freeway-arterial corridors.

3.3 Recommendation

After careful consideration and discussion with the project panel, the 6 candidate sites were reduced to two candidate sites: I-680 Northbound AM Peak with Capitol Ave. as the parallel arterial and I-680 Northbound AM Peak with Jackson Ave. as the parallel arterial. The other four candidate sites were not selected by the project team due to lack of cooperation from the local jurisdictions in charge of the arterial traffic signal operations. Finally, the project team decided to select I-680 Northbound AM Peak with Capitol Ave. as the parallel arterial. Both candidate sites share the same segment of freeway and both arterials have desirable road geometries, the site with Capitol Ave. as the parallel arterial is preferred due to the following reasons:

- Majority of the traffic heading onto the congested northbound direction of the freeway come from the east side of the freeway, which is the area surrounding Capitol Ave.
- City of San Jose strongly objected the inclusion of Jackson Ave as part of the corridor because various upgrades such as pedestrian signals and narrower road geometries have been planned in order to slow down traffic along the arterial and enhance pedestrian safety (Jackson Ave has relatively high volumes of pedestrian crossing and rates of pedestrian fatality).
  - o Future field tests may jeopardize pedestrian safety.
  - o improvements are unlikely due to pedestrian crossings rather than the interaction between freeway and arterial traffic becoming the major source of congestion on the arterial.

16

- Although there is concern about the transit signal priority (TSP) granted to the light rail vehicles that operate in the median of Capitol Ave, the relatively low frequency (every 15 minutes) and the field observations confirm that the TSP operation does not create operational issues.

Lastly, the project team was required to adjust the scope of the project in order to account for the lack of cooperation from Santa Clara County. The most upstream signalized intersection was removed from the study site due to the institutional constraints, and the most upstream freeway bottleneck (at Capitol Expy, on-ramp) was excluded. The finally selected study site is shown in Figure 3.7. It includes a three mile section of Northbound I-680 (post mile 1.65 to 4.48), and a segment of Capitol Ave parallel arterial with 5 signalized intersections.

The site selection process resulted in the best possible site among the available sites available sites. Also, it was a valuable experience in how to compromise between desired operating conditions (i.e. presence of bottlenecks) and practical constraints such as infrastructure, data availability and institutional barriers.

Figure 3.7 Map of Updated Study Site and Freeway Detector Locations

3.4 Details of the Selected Site

As shown in Figure 3.7, the selected site is a 3 mile section of I-680 from Alum Rock Ave. to Berryessa Rd. in San Jose, California. There are three recurrent bottlenecks on this stretch of I-680; they are located near the on-ramps from Berryessa Rd., McKee Rd., and Alum Rock Ave. At all three bottlenecks, high on-ramp demand from of the westbound direction of Berryessa Rd., McKee Rd., or Alum Rock Ave., along with high on-ramp demand from both directions of Capitol Ave., result in high volumes of merging traffic entering the northbound freeway mainline during the morning peak (7:30-9:30 AM).

One of the main reasons for morning peak demand in this stretch of highway is the increasing number of employment opportunities in the neighboring cities of Fremont and Milpitas. There are many trips generated from the densely populated residential areas surrounding San Jose in the south to the employment centers in Fremont and Milpitas in the north, during the morning peak period.

This section of the freeway has 4 lanes in each direction, whereas the parallel arterial Capitol Ave., as well as Alum Rock Ave. and Berryessa Rd. all have 2 lanes in each direction. McKee Rd. has 3 lanes in each direction. Typically, merging traffic from the arterial causes average speed to decrease to about 20 mph near the Alum Rock on-ramp, 30 mph near the McKee on-ramp, and 40 mph near the Berryessa on-ramp. Refer to Figure 3.8 for a contour plot of average speeds of the selected freeway segment during a typical morning peak, and Figures 3.9 to 3.11 for flow and speed time series of each bottleneck during a typical morning peak.
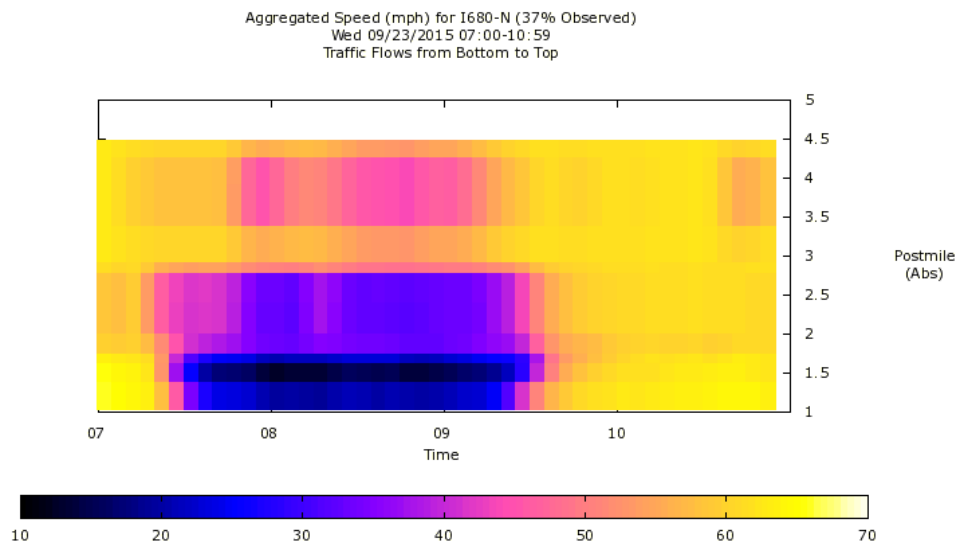
Figure 3.8: Speed Contour Plot of I-680 Northbound (Alum Rock Ave. to Berryessa Rd.)

18

Flow (Veh/5-Min)
144 Lane Points (100% Observed)
Mainline VDS 407176 - Alum Rock Rd rm-n-loop - I680-N
Wed 09/23/2015 07:00:00 to Wed 09/23/2015 13:59:59 (Hours=07:00-09:59)
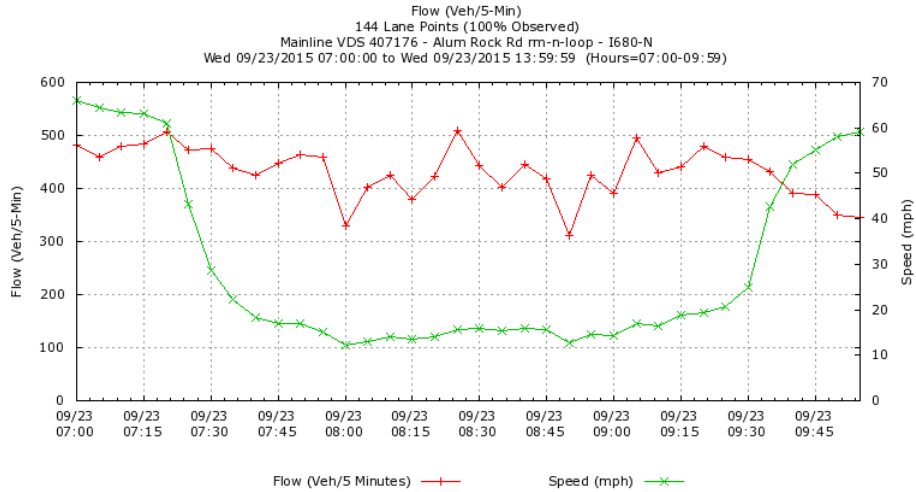
Figure 3.9 Flow and Speed of I-680 Northbound near Alum Rock Ave. On-ramp

Flow (Veh/5-Min)
144 Lane Points (100% Observed)
Mainline VDS 407179 - McKee Rd rm-n-diag - I680-N
Wed 09/23/2015 07:00:00 to Wed 09/23/2015 13:59:59 (Hours=07:00-09:59)
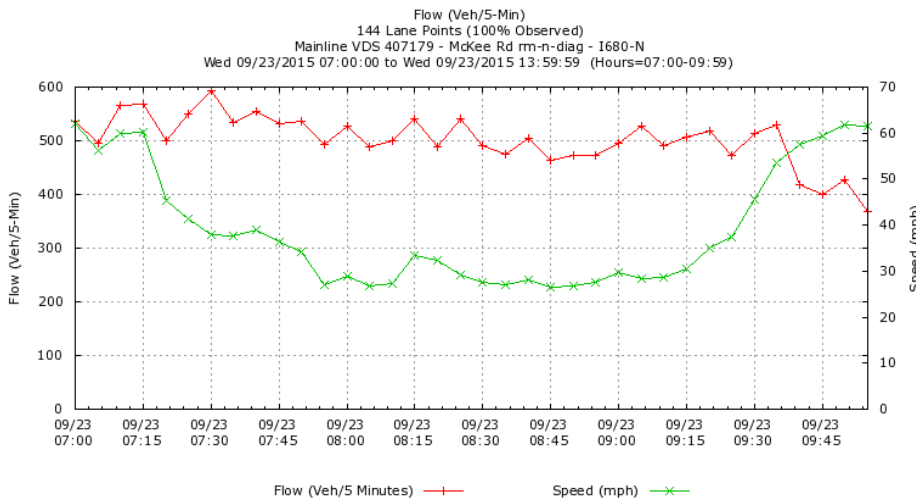
Figure 3.10: Flow and Speed of I-680 Northbound near McKee Rd. On-ramp

Flow (Veh/5-Min)
144 Lane Points (100% Observed)
Mainline VDS 407157 - Berryessa Rd rm-n-diag - I680-N
Wed 09/23/2015 07:00:00 to Wed 09/23/2015 13:59:59 (Hours=07:00-09:59)
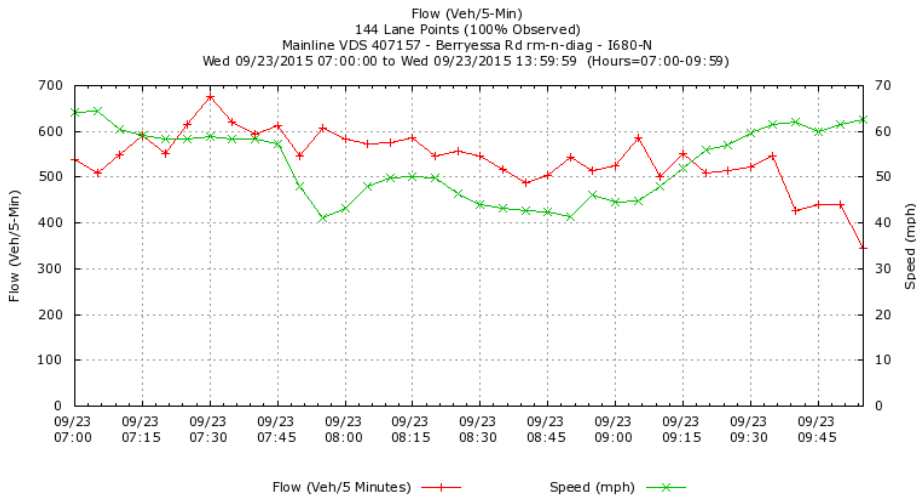
Figure 3.11: Flow and Speed of I-680 Northbound near Berryessa Rd. On-ramp

19

All of the on-ramps in this corridor are metered and the ramp meters operate under the local responsive demand-capacity approach. The metering rates are assigned based on various thresholds of freeway mainline occupancies immediately upstream of the merging or weaving area. The metering rates and their respective occupancy thresholds for each on-ramp are shown in Table 3.7 and Table 3.8.

The signalized intersections of this corridor operate with time of day (TOD) coordinated actuated timing plans. The existing cycle lengths are relatively long (130 to 160 seconds) and the signal timing plan provides progression to the northbound direction, which is the one with higher demand. Refer to Tables 3.12 to 3.15 for turning movement volumes and signal timing plans of the four major signalized intersections during a typical weekday morning peak.

Table 3.7: Alum Rock Ave. AM Peak Ramp Metering Rates

Time of Day	Alum Rock Ave. (loop)		Alum Rock Ave. (diagonal)	
	Mainline Occupancy	Meter Rate	Mainline Occupancy	Meter Rate
6:00 – 7:00 AM	≤ 3%	No metering	≤ 4%	No metering
	3% to 12%	900 vph/lane	4% to 14%	900 vph/lane
	≥ 12%	300 vph/lane	≥ 14%	560 vph/lane
7:00 – 7:30 AM	≤ 3%	No metering	≤ 4%	No metering
	3% to 5%	900 vph/lane	4% to 7%	900 vph/lane
	≥ 5%	300 vph/lane	≥ 7%	480 vph/lane
7:30 – 9:00 AM	≤ 3%	No metering	≤ 4%	No metering
	3% to 5%	900 vph/lane	4% to 7%	900 vph/lane
	≥ 5%	400 vph/lane	≥ 7%	480 vph/lane
9:00 – 10:00 AM	≤ 10%	No metering	≤ 12%	No metering
	10% to 12%	900 vph/lane	12% to 14%	900 vph/lane
	≥ 12%	360 vph/lane	≥ 14%	560 vph/lane

Table 3.8: McKee Rd. and Berryessa Rd. AM Peak Ramp Metering Rates

Time of Day	McKee Rd.		Berryessa Rd.	
	Mainline Occupancy	Meter Rate	Mainline Occupancy	Meter Rate
6:00 – 7:00 AM	≤ 4%	No metering	≤ 3%	No metering
	4% to 14%	900 vph/lane	3% to 14%	900 vph/lane
	≥ 14%	420 vph/lane	≥ 14%	420 vph/lane
7:00 – 7:15 AM	≤ 4%	No metering	≤ 3%	No metering
	4% to 6%	900 vph/lane	3% to 5%	900 vph/lane
	≥ 6%	400 vph/lane	≥ 5%	560 vph/lane
7:15 – 7:30 AM	≤ 4%	No metering	≤ 3%	No metering
	4% to 6%	900 vph/lane	3% to 5%	900 vph/lane
	≥ 6%	560 vph/lane	≥ 5%	560 vph/lane
7:30 – 7:45 AM	≤ 4%	No metering	≤ 3%	No metering
	4% to 6%	900 vph/lane	3% to 5%	900 vph/lane
	≥ 6%	720 vph/lane	≥ 5%	600 vph/lane
7:45 – 8:00 AM	≤ 4%	No metering	≤ 3%	No metering
	4% to 6%	900 vph/lane	3% to 5%	900 vph/lane
	≥ 6%	720 vph/lane	≥ 5%	650 vph/lane
8:00 – 8:15 AM	≤ 4%	No metering	≤ 3%	No metering
	4% to 6%	900 vph/lane	3% to 5%	900 vph/lane
	≥ 6%	600 vph/lane	≥ 5%	600 vph/lane
8:15 – 8:30 AM	≤ 4%	No metering	≤ 3%	No metering
	4% to 6%	900 vph/lane	3% to 5%	900 vph/lane
	≥ 6%	400 vph/lane	≥ 5%	600 vph/lane
8:30 – 9:00 AM	≤ 4%	No metering	≤ 3%	No metering
	4% to 6%	900 vph/lane	3% to 5%	900 vph/lane
	≥ 6%	400 vph/lane	≥ 5%	510 vph/lane
9:00 – 10:00 AM	≤ 12%	No metering	≤ 12%	No metering
	12% to 14%	900 vph/lane	12% to 14%	900 vph/lane
	≥ 14%	420 vph/lane	≥ 14%	450 vph/lane
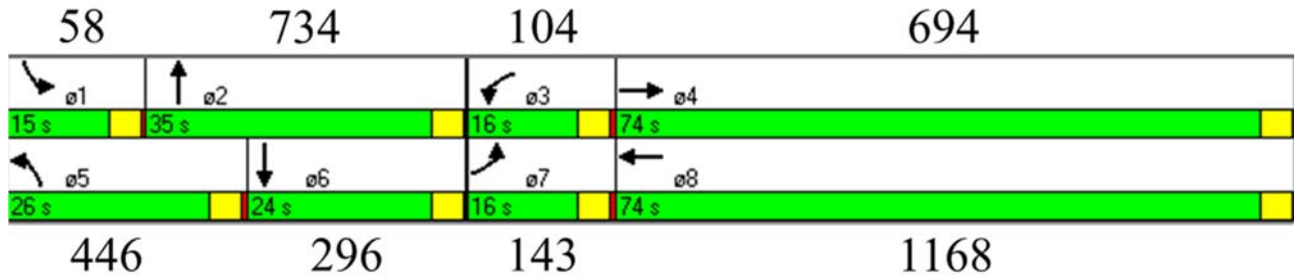
Figure 3.12: Signal Timing Plan and Typical Volumes at Capitol Ave. & Alum Rock Ave
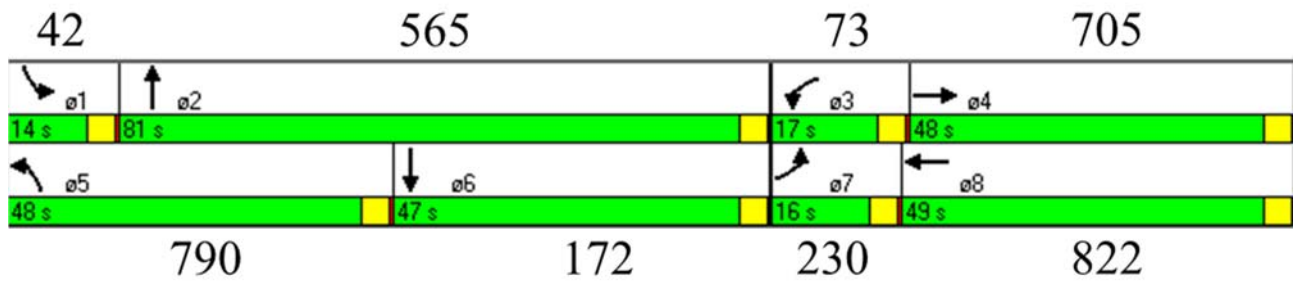
Figure 3.13: Signal Timing Plan and Typical Volumes at Capitol Ave. & Berryessa Rd
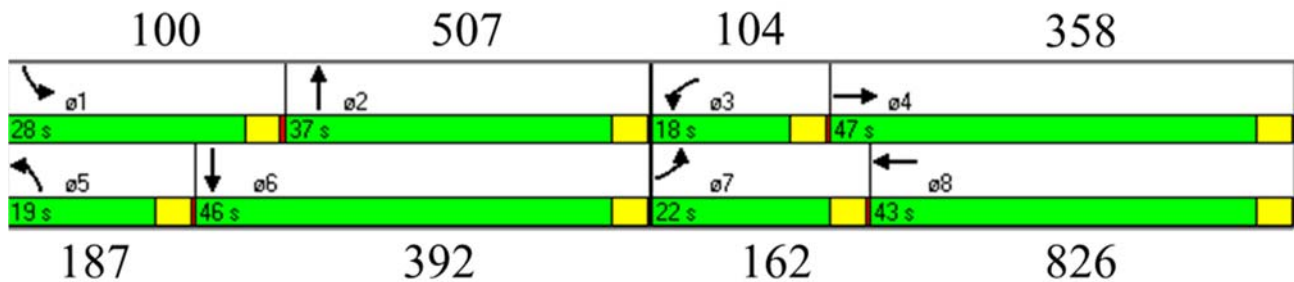
Figure 3.14: Signal Timing Plan and Typical Volumes at Capitol Ave. & Mabury Rd
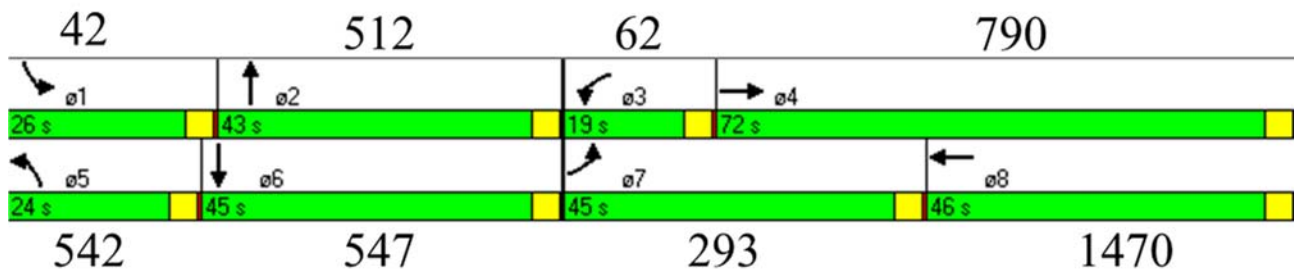
Figure 3.15: Signal Timing Plan and Typical Volumes at Capitol Ave. & McKee Rd

CHAPTER 4

PROPOSED CONTROL STRATEGIES FOR COORDINATION

Three control strategies were developed for coordinating freeway ramp metering and arterial traffic signals. The most appropriate and readily implementable control strategy was selected for extensive simulation tests and field implementation.

4.1 Control Strategy I: Ramp-Signal Control

This strategy is an extension of the control strategy developed by Su el al [12] in the previous research project (Coordination of Freeway Ramp Meters and Arterial Traffic Signals Phase I - Field Operational Test (FOT), Contract #65A0405) for coordination of a freeway ramp meter and a single signalized intersection. The algorithm was extended for arterial developed a control strategy for coordinating freeway ramp metering and arterial streets.

Freeway Ramp Metering

The ramp metering algorithm is intended to maximize freeway capacity by restricting the flow of on-ramp traffic. The ramp metering control adopted is a variation of ALINEA [13] known as UP ALINEA. This approach adapts ALINEA to scenarios in which the detectors are located immediately upstream of the merging area instead of immediately downstream of the merging area, as required by ALINEA.

Equation 4.1 shows how the ramp metering rates will be updated under ALINEA:

$$r(k) = r(k-1) + K_R[\hat{o} - o_{out}(k-1)] \tag{4.1}$$

where,

$r(k)$: metering rate at the k-th time interval
$\hat{o}$: desired occupancy, usually the value of critical occupancy
$o_{out}(k)$: occupancy measured immediately downstream of the on-ramp during the k-th time interval
K_R: regulator term

The ramp meter rate is updated every cycle, at same frequency as the detector measurements are updated. Typically, a cycle lasts 30 seconds.

For UP ALINEA, the occupancy downstream of the on-ramp is estimated instead of directly measured. The estimation is based on the occupancy measured upstream of the on-ramp, and the flows of the freeway mainlines and on-ramps. The estimation can be summarized as the following:

If the measured upstream occupancy is less than or equal to the critical occupancy, then the estimated downstream occupancy $\tilde{o}_{out}(k)$ is:

$$\tilde{o}_{out}(k) = \alpha o_{in}(k)\left(1 + \frac{q_r(k)}{q_{in}(k)}\right)\left(\frac{\lambda_{in}}{\lambda_{out}}\right) \tag{4.2}$$

where,

$o_{in}(k)$: occupancy measured immediately upstream of the on-ramp during the k-th time interval
$q_r(k)$: on-ramp flow during the k-th time interval
$q_{in}(k)$: freeway mainline flow during the k-th time interval

λ_{in}: number of lanes upstream of the on-ramp
λ_{out}: number of lanes downstream of the on-ramp
α: tuning parameter

Otherwise, the estimated downstream occupancy $\tilde{o}_{out}(k)$ would be:

$$\tilde{o}_{out}(k) = \gamma \tilde{o}'_{in}(k) + (1 - \gamma)\tilde{o}'_{in}(k - 1) \tag{4.3}$$

where,

$$\tilde{o}'_{in}(k) = \tilde{o}_{in}(k) \cdot \frac{\lambda_{in}}{\lambda_{out}} + \frac{100L}{w\lambda_{out}} \cdot q_r(k)$$

w: shockwave speed
γ: tuning parameter
L: section length

Lastly, this proposed control for ramp metering does not incorporate queue override.

Arterial Traffic Signals

According to the work done in Phase I, the coordination strategy for an isolated arterial intersection adjacent to a freeway interchange balances the demand and supply of the green time of each phase while taking the capacity and queue length of the on-ramp into account, using a linear optimization model. The model assumes uniform arrivals, fixed phase sequence, constant lane capacities, and sufficient queue storage space downstream of the intersection unless a freeway on-ramp is located downstream. The objective function of the optimization model is shown in equation 4.4.

$$Min \sum_{i \neq j} \mu_{ij} \left| \frac{g_i(T)}{\frac{q_i(T-1) + d_i(T) \cdot C}{f_{sat,i}}} - v_{ij} \left(\frac{g_j(T)}{\frac{q_j(T-1) + d_j(T) \cdot C}{f_{sat,j}}} \right) \right|$$
$$+ \delta \left| \sum_r \left(\sum_{i \in R} f_{sat,i} \cdot g_i(T) \cdot \beta_i - (RA_r + RA_l) \right) \right| \tag{4.4}$$

where,

$g_i(T)$: decision variable; optimal green time of phase i and the T-th cycle
C: cycle length
$d_i(T)$: uniform traffic demand (arrival rate) during the T-th cycle
$q_i(T)$: residual queue length at the end of the T-th cycle
$f_{sat,i}$ saturation flow of phase i
R: indication that the downstream section of phase i has access to an on-ramp
β_i: proportion of the traffic in phase i that accesses the on-ramp (based on historical data)
RA_r: available on-ramp storage space of ramp r
RA_l: available storage space of the arterial lanes with on-ramp access
μ_{ij}, v_{ij}: tuning parameters for phase prioritization
δ: weighting factor for the penalty function.

The cycle length is assumed to be known in advance and is typically the network-wide optimal cycle length used in the coordinated actuated arterial traffic signals. $q_i(T)$, RA_r, and RA_l can be estimated by computing

the difference between the number of arrivals upstream and the number of departures downstream during the previous cycle.

The expression

$$\frac{q_i(T-1) + d_i(T) \cdot C}{f_{sat,i}}$$

is the demand of green time of phase i in cycle T, and $g_i(T)$ is the supply of green time of phase i in cycle T.

The expression $\sum_{i \in R} f_{sat,ik} \cdot g_i(t) \cdot \beta_i$ is the maximum flow discharged toward freeway on-ramp r from the adjacent intersection. The objective function penalizes the difference between the total flow discharged from the adjacent intersection and the sum of RA_r and RA_l, as illustrated in Figure 4.1. This penalty function is intended to reduce green times to the turning movements that discharge traffic onto on-ramp r when on-ramp r and the adjacent arterial lanes for on-ramp access can no longer accommodate the demand. This would reallocate the green times to the conflicting directions. Furthermore, this would mitigate the queue spillback of the freeway on-ramp and its immediate upstream areas thus prevent on-ramp traffic from blocking the intersection and therefore the need for queue override. As a result, the absence of queue override would prevent any further negative impact on the freeway performance.
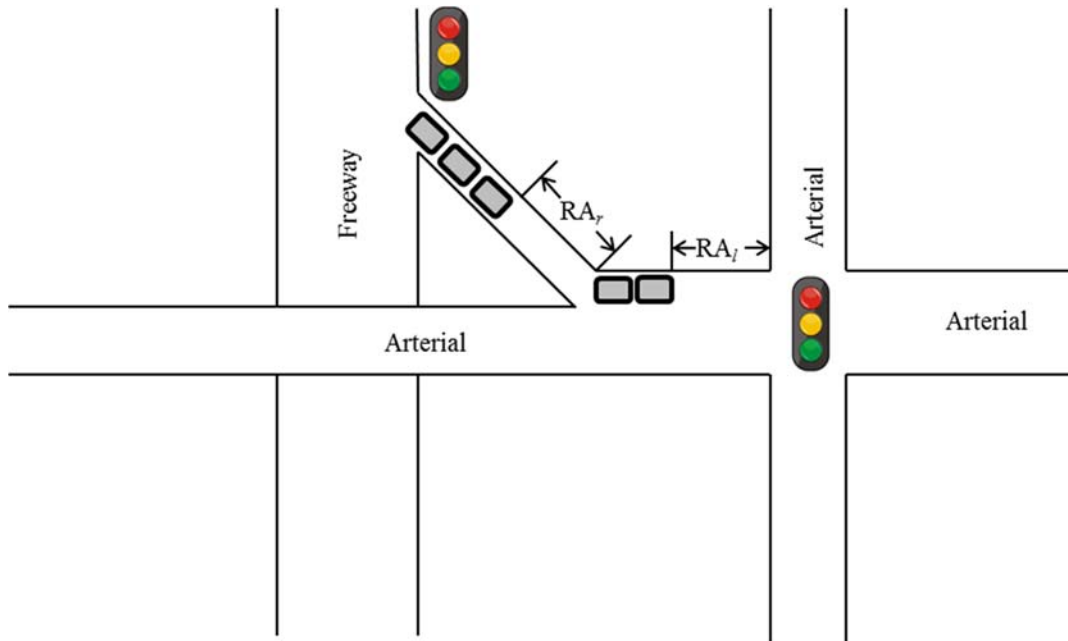
Figure 4.1 Arterial and Freeway On-ramp Queues

Equations 4.5 to 4.7 are the constraints that address several practical limitations; equation 4.5 ensures that the minimum green time $G_{i,min}$ of phase i related to traffic safety is satisfied, and equations 4.6 and 4.7 ensures that the dual ring structure is followed.

$$g_i(T) \geq G_{i,min} \tag{4.5}$$

$$g_1(T) + g_2(T) = g_5(T) + g_6(T) \tag{4.6}$$

$$\sum_{i=1-4 \text{ or } 5-8} g_i(t) = C \tag{4.7}$$

Modification after Phase I

In order for the approach presented in Phase I to be applicable at a corridor level, the interaction between adjacent signalized intersections must be considered. Thus, a new penalty term was added to the objective function presented in Phase I. The additional penalty term is the following:

$$\varepsilon \left| \sum_{i \in AR} \left(f_{sat,ik} \cdot [o_{ik}(T) + l_{acc}] - \left[s_L - \sum_{i \in L} q_{i,k+1}(T) \right] \right) \right| \tag{4.8}$$

where,

$o_{ik}(T)$: offset between phase i of intersection k and the corresponding phase in the downstream intersection during the T-th cycle
l_{acc}: start-up lost time
s_L: length of the downstream link (in number of vehicles)
$q_{i,k+1}(T)$: queue length of phase i of the downstream intersection at the end of cycle T
AR: indication that the downstream section is an arterial
L: indicator for the downstream arterial link
ε: weighting factor for the penalty function

Figure 4.2 provides an illustration of the notations shown in Equation 4.8.
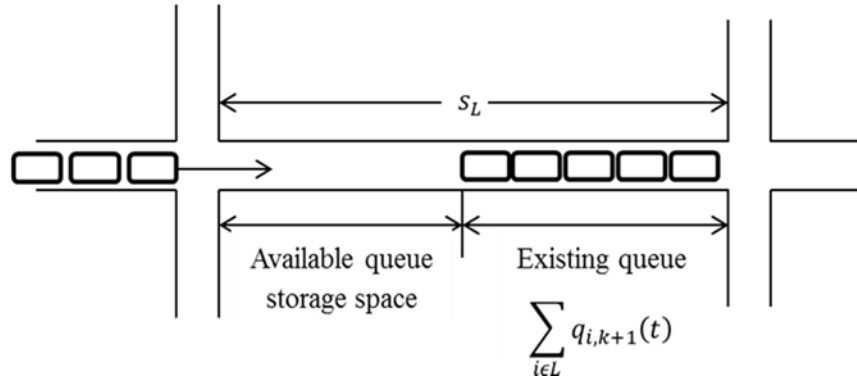
Figure 4.2 Queues at Adjacent Signalized Intersections

For adjacent signalized intersections, the offset between the corresponding phases of the upstream and downstream intersections causes the downstream intersection to initiate green at a later time, thus during the time between the beginning of green of phase i of intersection k and the beginning of green of the corresponding phase in the downstream intersection, the flow through phase i of intersection k is $f_{sat,ik} \cdot [o_{ik}(T) + l_{acc}]$. In order to reduce the upstream green time when the downstream section cannot accommodate the flow discharged from the upstream intersection, the control strategy penalizes on the difference between the flow discharged upstream and the amount of queue storage space downstream so that more green time would be allocated to the conflicting directions instead. Thus, the new optimization model is formulated as the following:

$$Min \sum_{i \neq j} \mu_{ij} \left| \frac{g_i(T)}{\frac{q_i(T-1) + d_i(T) \cdot C}{f_{sat,i}}} - v_{ij} \left(\frac{g_j(T)}{\frac{q_j(T-1) + d_j(T) \cdot C}{f_{sat,j}}} \right) \right|$$

$$+ \delta \left| \sum_r \left(\sum_{i \in R} f_{sat,i} \cdot g_i(T) \cdot \beta_i - (RA_r + RA_l) \right) \right| \tag{4.9}$$

$$+ \varepsilon \left| \sum_{i \in AR} \left(f_{sat,ik} \cdot [o_{ik}(T) + l_{acc}] - \left[s_L - \sum_{i \in L} q_{i,k+1}(T) \right] \right) \right|$$

Subject to:

$$g_i(T) \geq G_{i,min} \tag{4.10}$$

$$g_1(T) + g_2(T) = g_5(T) + g_6(T) \tag{4.11}$$

$$\sum_{i=1-4 \ or \ 5-8} g_i(t) = C \tag{4.12}$$

However, this coordination strategy has its limitation because the arterial traffic signals are optimized under the less realistic assumption that vehicles arrive uniformly at the intersection. With signalized intersections nearby, this assumption no longer holds due to the fact that the time and distribution of arrivals from the upstream intersection depend heavily on the time at which the green phase begins and the duration of the green phase at the upstream intersection. Typically, traffic from the upstream intersection arrives in platoons during a short time interval instead of uniformly over a longer period of time. As a result, the misrepresentation of arrival pattern could have increased the delay of each turning movement at the selected intersection. Furthermore, this limitation would lead to less optimal results in the analysis of an arterial corridor as well. In order to address this limitation, a new coordination strategy was developed and is discussed in the next section.

4.2 Control Strategy II: Arterial Green Time Re-allocation

A new control strategy was developed to address the limitation of the previous method for signal optimization. In addition, the coordination strategy is no longer restricted to implementing ALINEA as the freeway ramp metering algorithm.

Freeway Ramp Metering

Unlike the previous control strategy, this proposed control strategy for coordinating arterial traffic signals and freeway ramp metering is not limited to any specific freeway ramp metering algorithm. Thus, the ramp metering algorithm does not have to be modified. The only change is the deactivation of queue override that is designed to releases on-ramp queues onto the freeway to prevent spillback, and this was neglected in the previous control strategy.

With better arterial signal timing designed to prevent queue spillback and mitigate unnecessary penalties, the freeway ramp meter no longer needs queue override because the arterial traffic signals can now compensate for the negative impact of on-ramp queues on nearby arterials as a result of metering freeway on-ramps restrictively. This would mitigate the capacity drop as a result of releasing on-ramp queue on the freeway.

Arterial Traffic Signals

A new control strategy for the signalized intersections near the freeway on-ramps was developed. According to this strategy, signal timings are optimized for all signalized intersections along the arterial every cycle, in order to minimize delay. Similar to the original coordination strategy, the cycle is assumed to be known in advance.

The following notations will be used:

u: intersection index
$g_{i,T}^u$: green time allocated to phase i in cycle T at intersection u [sec]
$g_{i,min}^u$: minimum green time of phase i at intersection u [sec]
$g_{i,max}^u$: maximum green time of phase i at intersection u [sec]
I^u: total number of phases in a cycle for intersection u
L^u: total lost time at intersection u [sec]
C: cycle length [sec]
$R_j^{(1)u}(g_{i,T}^u)$: red time from the beginning of the cycle to the beginning of the green for the subject lane group
$G_j^{e,u}(g_{i,T}^u)$: duration of effective green time for the subject lane group
$R_j^{(2)u}(g_{i,T}^u)$: red time from the end of the green to the end of the cycle for the subject lane group

$$R_j^{(1)u}(g_{i,T}^u) = \sum_{i=1}^{k_j^u-1} g_{i,T}^u + \sum_{i=1}^{k_j^u-1} y_i^u$$

$$G_j^{e,u}(g_{i,T}^u) = \sum_{i=k_j^u}^{l_j^u} g_{i,T}^u + \sum_{i=k_j^u}^{l_j^u-1} y_i^u$$

$$R_j^{(2)u}(g_{i,T}^u) = \sum_{i=l_j^u+1}^{I^u} g_{i,T}^u + \sum_{i=l_j^u}^{I^u} y_i^u$$

y_i^u: yellow time interval after phase i at intersection u
$g_{i,T}^u$: green time for phase i in cycle T at intersection u
k_j^u: the first phase in a cycle that can serve lane group i at intersection u
l_j^u: the last phase in a cycle that can serve lane group i at intersection u

The new optimization model is the following:

Minimize

$$\sum_{u=1}^{N_i}\sum_{j=1}^{J_u}(D_{j,T}^{H,u} + D_{j,T}^{T,u}) + \sum_{u=1}^{N_i}\sum_{j=1}^{J_u} D_{j,T}^{Q,u} + \sum_{r=1}^{N_r} D_T^r \tag{4.13}$$

Subject to:

$$g_{i,min}^u \leq g_{i,T}^u \leq g_{i,max}^u \tag{4.14}$$

$$\sum_{i=1}^{I^u} g_{i,T}^u + L^u = C \tag{4.15}$$

$$N_T^r \leq RS_r \tag{4.16}$$

The objective function, shown in equation 4.13, consists of the delay at the signalized intersections and the delay at the freeway on-ramps. The delay at the signalized intersection includes the delay for vehicles that travel in platoons on incoming links and the delay for vehicles in residuals queues. $D_{j,T}^{H,u}$ and $D_{j,T}^{T,u}$ denote the delays caused by stopping the head and tail of the platoon, respectively, $D_{j,T}^{Q,u}$ is the delay experienced by vehicles in the residual queues, D_T^r is the delay experienced by vehicles on the on-ramps, N_i is the number of signalized intersections along the arterial, N_r is the number of on-ramps in the system, and J_u is the number of lane groups at intersection u. These delays are expressed as functions of the optimal green times, which are the decision variables. The optimal green times also determine the beginning of the coordinated phase, which is typically the arterial's through movement.

There are several constraints. Equation 4.14 is a constraint for maximum and minimum allowable green time, Equation 4.15 is a constraint that ensures the sum of all green times equals the cycle length, and Equation 4.16 is a constraint that ensures the number of vehicles in the residual queue of on-ramp r at the end of cycle T, N_T^r, does not exceed RS_r, which is the number of vehicles that on-ramp r can accommodate at jam density.

The delays at the signalized intersections are estimated under the assumption of deterministic vehicle arrivals, fixed phase sequences, constant lane capacities, and negligible platoon dispersion. Thus, the vehicles arrive and are served at the intersection at capacity, and that all vehicle trajectories are parallel assuming that kinematic wave theory [14, 15] holds. This implies that the first and last vehicle that get stopped in a platoon will experience the same delay, thus the total delay of all vehicles can be easily calculated using only the arrival time of the first vehicle in a platoon at the back of its lane group's queue at intersection u, $t_{j,T}^u$, the size of the platoon, $P_{j,T}^u$, and the traffic conditions at the approach as expressed by the size of the residual queue of lane group j at the end of the previous cycle $T - 1$, $N_{j,T-1}^u$. The size of the platoon in lane group j at intersection, u, during cycle T, $P_{j,T}^u$ can be determined using the sum of the flows of all movements that discharge traffic toward intersection u during the last cycle, which can be measured by the stop line detectors on the corresponding lanes of the upstream intersection, assuming there are reasonable estimates of the percentages of traffic choosing the left turn, thru, and right turn lanes at intersection u.

For simplicity and ease of computation, the delay calculations are done under the assumption of single platoon, however, the control strategy could be extended to include multiple platoons arriving within a cycle. For the arrival time of the first vehicle in a platoon at the back of lane group j's queue at intersection u, $t_{j,T}^u$, the sum of the time at which the first vehicle of the upstream intersection's first phase or turning movement that discharges vehicle toward intersection u leaves the stop bar detector and the free-flow travel time from the upstream intersection to intersection u would provide an accurate estimate. With an accurate estimate of the platoon arrival time, the effect of disruption of the progression can be accounted for in the delay estimation. However, in order to optimize multiple signals at the same time, the arrival time of the platoon and the start time of the cycle must be normalized by the free-flow travel time from each intersection to the critical intersection, a method known as coordinate transformation proposed by Newell [16]. Lastly,

the size of the residual queue of lane group j at the end of the previous cycle $T - 1$, $N_{j,T-1}^u$, can be calculated using the measured parameters. In summary, the delay estimation requires minimal field measurements, and the measurements can be obtained using existing loop detectors commonly placed at the stop bars of the signalized intersections.

The delay estimations for signalized intersections vary on a case-by-case basis, and can be calculated based on the details shown below. In order to determine which of the cases is applicable, a binary decision variable and the related constraints for time of platoon arrival and residual queue can be introduced, and the summation of the binary variables for a lane group should be constrained to one in order to apply only one delay equation for each lane group of a signalized intersection.

Case 1: Arrival before residual queue served, entire platoon served in green

A platoon of size $P_{j,T}^u$ that belongs to lane group j of intersection u arrives at the back of its lane group's queue during cycle T at time $t_{j,T}^u$ before the time that the corresponding residual queue of j from the previous cycle $T - 1$, $N_{j,T-1}^u$, would have finished being served if there was enough green time available. There is enough available green time to serve the residual queue, and spare green time to serve all $P_{j,T}^u$ vehicles in the platoon. These conditions are summarized as:

$$t_{j,T}^u \leq t_T^u + R_j^{(1)u}(g_{i,T}^u) + \frac{N_{j,T-1}^u}{s_j^u}$$

$$N_{j,T-1}^u \leq G_j^{e,u}(g_{i,T}^u)s_j^u$$

$$P_{j,T}^u \leq G_j^{e,u}(g_{i,T}^u)s_j^u - N_{j,T-1}^u$$

where s_j^u is the saturation flow for lane group j at intersection u and t_T^u is the beginning of cycle T for intersection u, normalized by the free-flow travel time between intersection u and the critical intersection, which is determined as:

$$t_T^u = t_T + O_T^u - \frac{d_{cr}^u}{v_f}$$

$t_T = (T - 1)C$ is the beginning of cycle T at the critical intersection which is the first one to be optimized and O_T^u is the difference between the starting time of cycle T at intersection u and the critical intersection, normalized by the free-flow travel time of between intersection u and the critical intersection. The number of vehicles in the residual queue, $N_{j,T-1}^u$, is calculated as:

$$N_{j,T-1}^u = \max\{P_{j,T-1}^u + N_{j,T-2}^u - G_j^{e,u}(g_{i,T-1}^u)s_j^u, 0\}$$

As shown in Figure 4.3, all vehicles in the platoon experience delay caused by stopping the head of the platoon, $D_{j,T}^{H,u}$:

$$D_{j,T}^{H,u} = P_{j,T}^u \left(t_T^u + R_j^{(1)u}(g_{i,T}^u) + \frac{N_{j,T-1}^u}{s_j^u} - t_{j,T}^u \right)$$

but no delay caused by stopping the tail of the platoon, $D_{j,T}^{T,u}$.
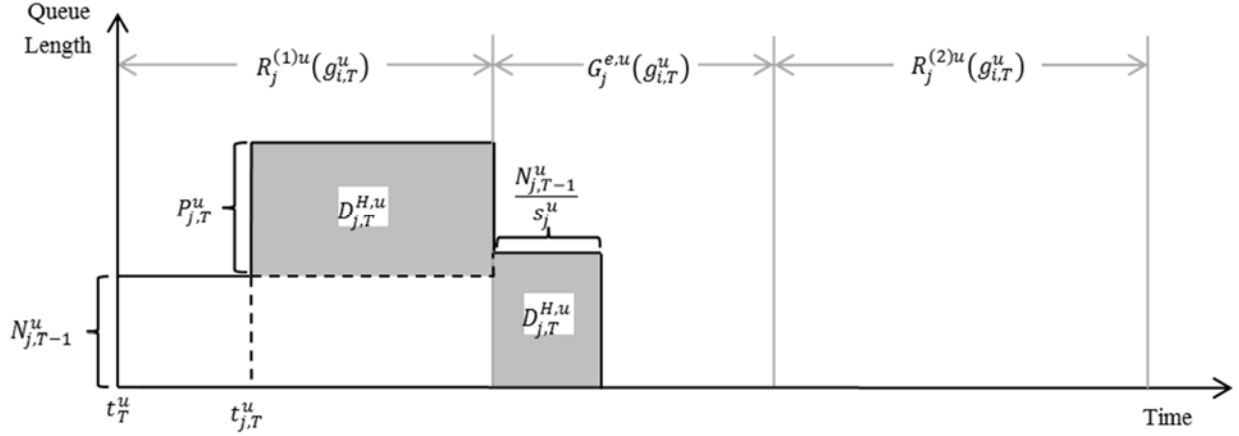
Figure 4.3 Delay of Platoon in Case 1

Case 2: Arrival before residual queue served, insufficient green to serve entire platoon

A platoon of size $P_{j,T}^u$ arrives at the back of its lane group's queue at time $t_{j,T}^u$ before the time that the corresponding residual queue $N_{j,T-1}^u$, would have finished being served. There is enough available green time to serve the residual queue, but there is not enough spare green time to serve all $P_{j,T}^u$ vehicles. These conditions are summarized as:

$$t_{j,T}^u \leq t_T^u + R_j^{(1)u}(g_{i,T}^u) + \frac{N_{j,T-1}^u}{s_j^u}$$

$$N_{j,T-1}^u \leq G_j^{e,u}(g_{i,T}^u)s_j^u$$

$$P_{j,T}^u \geq G_j^{e,u}(g_{i,T}^u)s_j^u - N_{j,T-1}^u$$

According to Figure 4.4, all vehicles in the platoon experience delay caused by stopping the head of the platoon, $D_{j,T}^{H,u}$, and a portion of the vehicles experience delay caused by stopping the tail of the platoon, $D_{j,T}^{T,u}$:

$$D_{j,T}^{H,u} = P_{j,T}^u \left(t_T^u + R_j^{(1)u}(g_{i,T}^u) + \frac{N_{j,T-1}^u}{s_j^u} - t_{j,T}^u \right)$$

$$D_{j,T}^{T,u} = \left(P_{j,T}^u - G_j^{e,u}(g_{i,T}^u)s_j^u + N_{j,T-1}^u \right)\left(C - \frac{N_{j,T-1}^u}{s_j^u} \right)$$

For linearity, the delay caused by stopping the tail of the platoon is equal to the cycle length minus the time it takes to serve the residual queue. Although this overestimates the delay caused by stopping the tail of the platoon by $R_j^{(1)u}(g_{i,T}^u)$, it maintains computational simplicity.
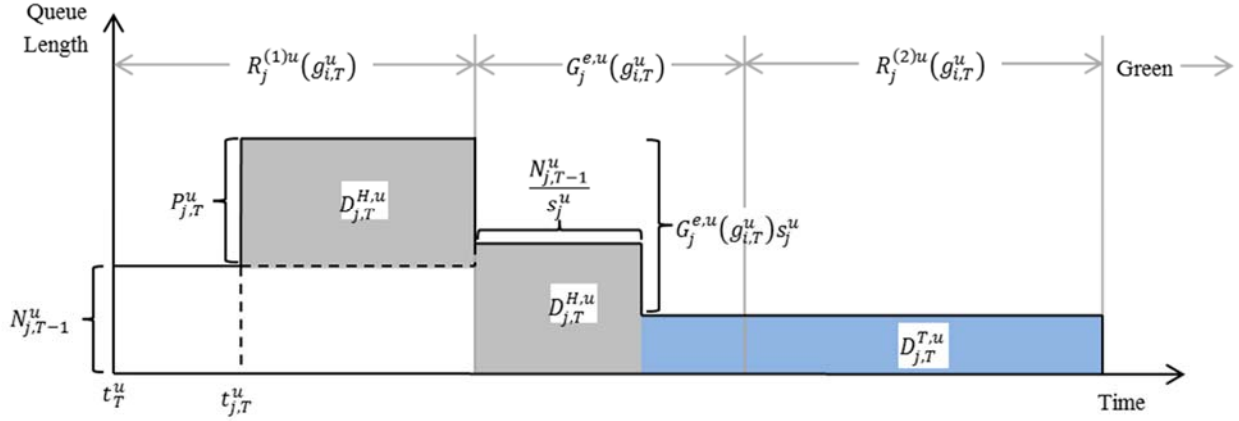
Figure 4.4 Delay of Platoon in Case 2

Case 3: Arrival before end of green, insufficient green to serve residual queue

A platoon of size $P_{j,T}^u$ arrives at the back of its lane group's queue at time $t_{j,T}^u$, before the end of the phase that can serve it, but there is not enough available green time to serve all $N_{j,T-1}^u$ vehicles in the residual queue. These conditions are summarized as:

$$t_{j,T}^u \leq t_T^u + R_j^{(1)u}\big(g_{i,T}^u\big) + G_j^{e,u}\big(g_{i,T}^u\big)$$

$$N_{j,T-1}^u \geq G_j^{e,u}\big(g_{i,T}^u\big)s_j^u$$

As shown in Figure 4.5, all vehicles in the platoon experience delay caused by stopping the head of the platoon. $D_{j,T}^{H,u}$, and by stopping the tail of the platoon, $D_{j,T}^{T,u}$:

$$D_{j,T}^{H,u} = P_{j,T}^u \left(t_T^u + R_j^{(1)u}\big(g_{i,T}^u\big) + G_j^{e,u}\big(g_{i,T}^u\big) - t_{j,T}^u\right)$$

$$D_{j,T}^{T,u} = P_{j,T}^u \left(R_j^{(2)u}\big(g_{i,T}^u\big)\right)$$
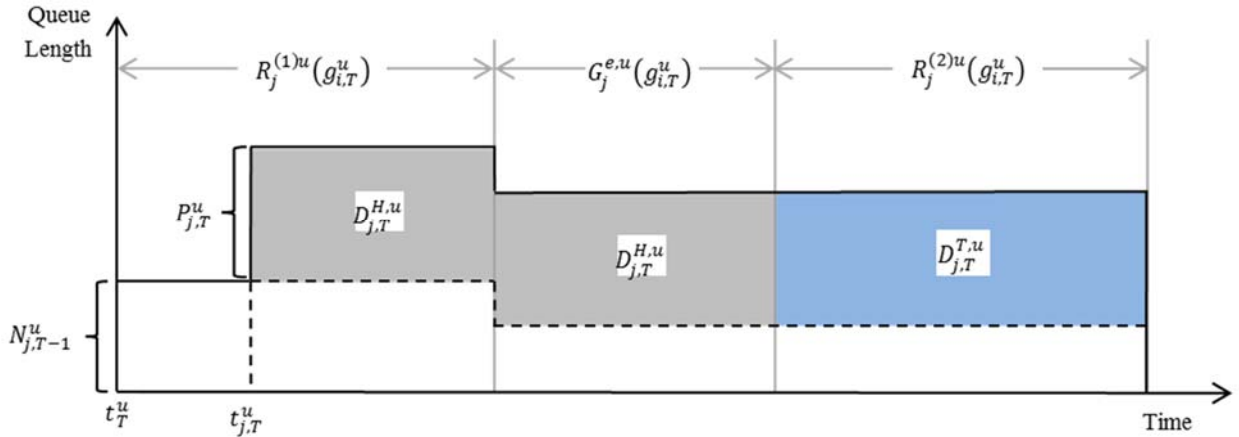
Figure 4.5 Delay of Platoon in Case 3

32

Case 4: Arrival after residual queue served, entire platoon served in green

A platoon of size $P_{j,T}^u$ arrives at the back of its lane group's queue at time $t_{j,T}^u$ after the time that the corresponding residual queue $N_{j,T-1}^u$, would have finished being served. There is enough available green time to serve the residual queue, and there is enough spare green time to serve all $P_{j,T}^u$ vehicles. These conditions are summarized as:

$$t_{j,T}^u \geq t_T^u + R_j^{(1)u}(g_{i,T}^u) + \frac{N_{j,T-1}^u}{s_j^u}$$

$$N_{j,T-1}^u \leq G_j^{e,u}(g_{i,T}^u)s_j^u$$

$$P_{j,T}^u \leq \left(t_T^u + R_j^{(1)u}(g_{i,T}^u) + G_j^{e,u}(g_{i,T}^u) - t_{j,T}^u\right)s_j^u$$

In this case, vehicles in the platoon do not experience any delay at intersection u. As a result, both the delay caused by stopping the head of that platoon, $D_{j,T}^{H,u}$, and by stopping the tail of the platoon, $D_{j,T}^{T,u}$, are zero, as illustrated in Figure 4.6.
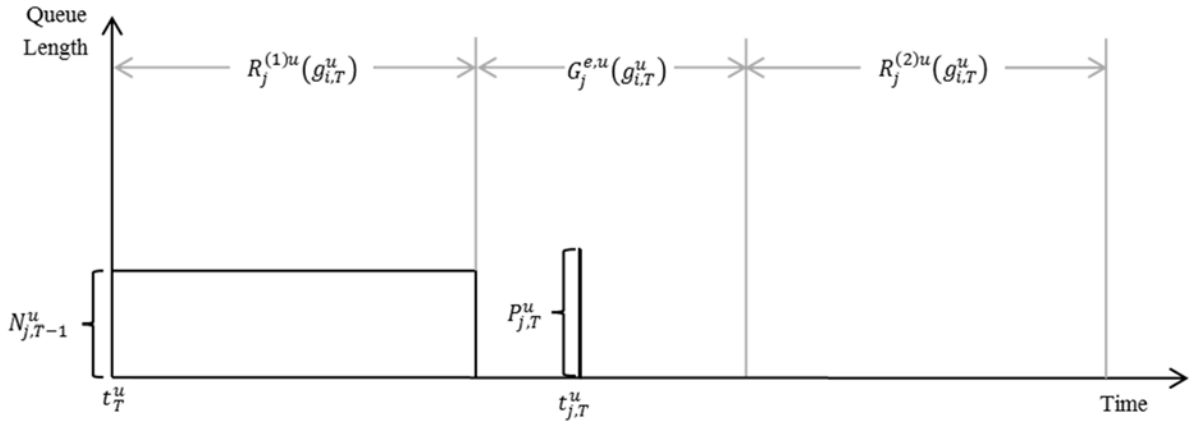
Figure 4.6 Delay of Platoon in Case 4

Case 5: Arrival after residual queue served, insufficient green to serve entire platoon

A platoon of size $P_{j,T}^u$ arrives at the back of its lane group's queue at time $t_{j,T}^u$ after the time that the corresponding residual queue, $N_{j,T-1}^u$, would have finished being served. There is enough available green time to serve the residual queue, but there is not enough spare green time to serve all $P_{j,T}^u$ vehicles. These conditions are summarized as:

$$t_{j,T}^u \geq t_T^u + R_j^{(1)u}(g_{i,T}^u) + \frac{N_{j,T-1}^u}{s_j^u}$$

$$N_{j,T-1}^u \leq G_j^{e,u}(g_{i,T}^u)s_j^u$$

$$P_{j,T}^u \geq \left(t_T^u + R_j^{(1)u}(g_{i,T}^u) + G_j^{e,u}(g_{i,T}^u) - t_{j,T}^u\right)s_j^u$$

A portion of vehicles in the platoon experience delay caused by stopping the tail of the platoon, $D_{j,T}^{T,u}$:

$$D_{j,T}^{T,u} = \left[P_{j,T}^u - \left(t_T^u + R_j^{(1)u}(g_{i,T}^u) + G_j^{e,u}(g_{i,T}^u) - t_{j,T}^u \right) s_j^u \right] \left(t_{T+1}^u - t_{j,T}^u \right)$$

but no delay caused by stopping the head of the platoon, $D_{j,T}^{H,u}$, shown in Figure 4.7. This portion of vehicles in the platoon will also experience residual queue delay in the next cycle.
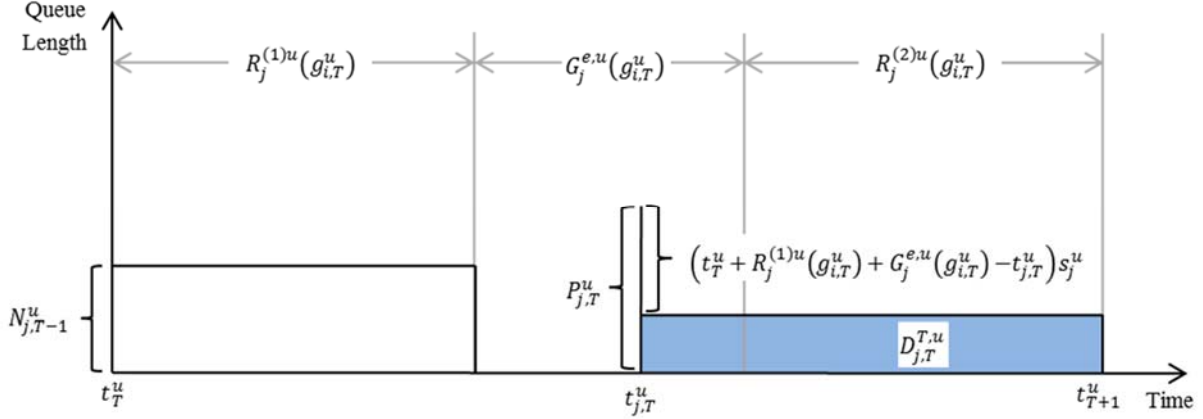
Figure 4.7 Delay of platoon in Case 5

Case 6: Arrival after the green

A platoon of size $P_{j,T}^u$ arrives at the back of its lane group's queue at time $t_{j,T}^u$ after the end of the phase that can serve it. This case captures all arrivals not satisfying the conditions of cases 1 through 5, and it can all be expressed as

$$t_{j,T}^u > t_T^u + R_j^{(1)u}(g_{i,T}^u) + G_j^{e,u}(g_{i,T}^u)$$

All vehicles in the platoon experience delay caused by stopping the tail of the platoon, $D_{j,T}^{T,u}$:

$$D_{j,T}^{T,u} = P_{j,T}^u \left(t_{T+1}^u - t_{j,T}^u \right)$$

but no delay caused by stopping the head of the platoon, $D_{j,T}^{H,u}$, as illustrated in Figure 4.8.
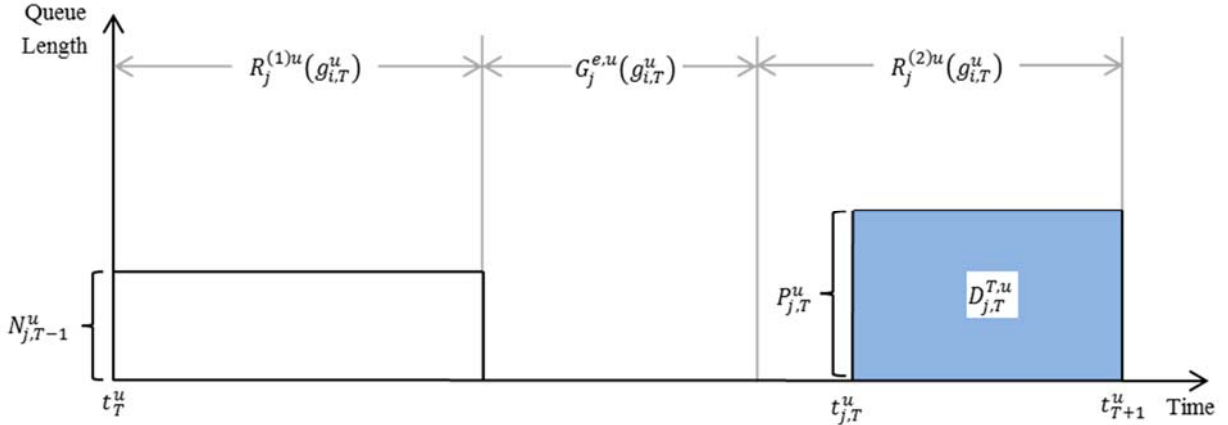
Figure 4.8 Delay of Platoon in Case 6

34

The delay for vehicles in residual queues at signalized intersections are estimated based on the size of the residual queue and whether or not it can be entirely served during cycle T. Two cases arise which are described next along with the corresponding delay equations for an intersection u:

Case A: Residual queue served in green

The residual queue of a lane group j, $N_{j,T-1}^u$, can be entirely served during cycle T:

$$N_{j,T-1}^u \leq G_j^{e,u}(g_{i,T}^u)s_j^u$$

Shown in Figure 4.9, the total delay experienced by all vehicles in the residual queue, $D_{j,T}^{Q,u}$, is

$$D_{j,T}^{Q,u} = N_{j,T-1}^u R_j^{(1)u}(g_{i,T}^u)$$
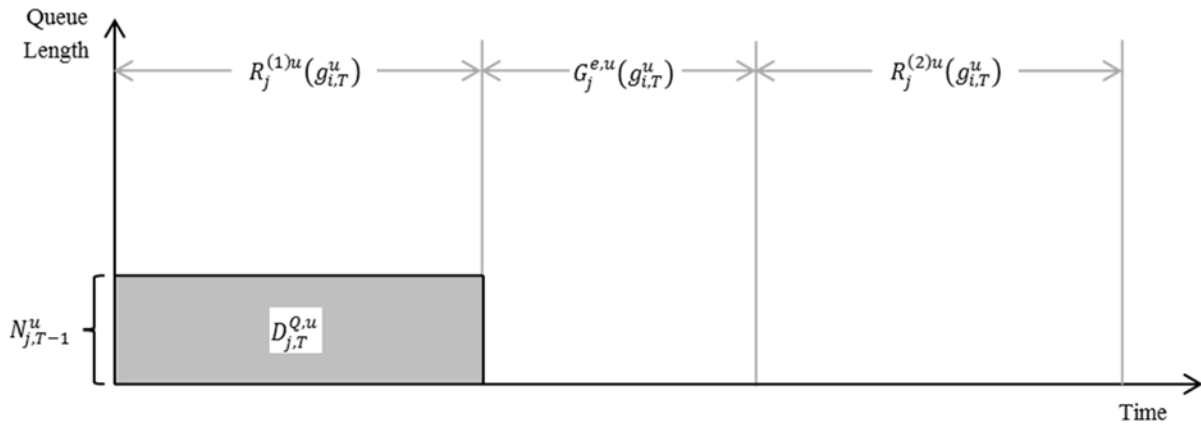
Figure 4.9 Residual Queue Delay of Case A

Case B: Residual queue not entirely served in green

The residual queue of a lane group j, $N_{j,T-1}^u$, cannot be entirely served during cycle T:

$$N_{j,T-1}^u \geq G_j^{e,u}(g_{i,T}^u)s_j^u$$

Shown in Figure 4.10, the total delay experienced by all vehicles in the residual queue, $D_{j,T}^{Q,u}$, is:

$$D_{j,T}^{Q,u} = N_{j,T-1}^u R_j^{(1)u}(g_{i,T}^u) + \left(N_{j,T-1}^u - G_j^{e,u}(g_{i,T}^u)s_j^u\right)C$$

because the vehicles that do not get served will have to wait for an extra cycle before they start being served.
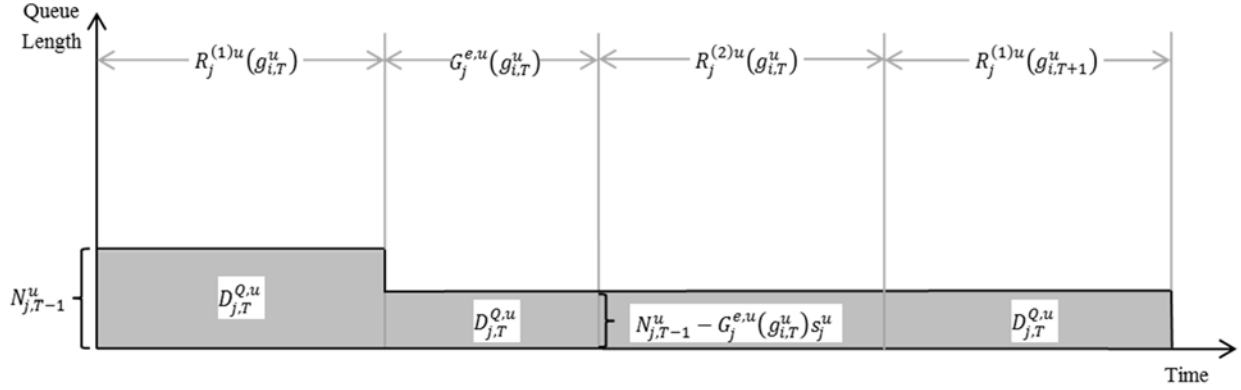
Figure 4.10 Residual Queue Delay of Case B

The delay incurred by vehicles at the freeway on-ramps is determined by the number of vehicles discharged at the ramp meter, the number of vehicles already queuing on the freeway on-ramp, and the number of vehicles arrived at the ramp meter, and those that cannot be discharged during cycle T incur delays equivalent to the duration of the entire cycle. The delay at the freeway on-ramp, D_T^r can be expressed as:

$$D_T^r = \left[\left(\sum_{j \in ramp} G_j^{e,u}(g_{i,T}^u)s_j^u \right) + N_{T-1}^r - RM_T^r \cdot C \right] C$$

where $\sum_{j \in ramp} G_j^{e,u}(g_{i,T}^u)s_j^u$ is the number of vehicles discharged from the corresponding lane groups at the upstream signalized intersection to the freeway on-ramp r, during cycle T. RM_T^r is the ramp meter rate of freeway on-ramp r during cycle T, and C is the duration of the cycle T. The residual queue from the last cycle N_{T-1}^r can be calculated using the following expression:

$$N_{T-1}^r = \left(\sum_{j \in ramp} P_{j,T-1}^u \right) + N_{j,T-2}^r - RM_{T-1}^r \cdot C$$

where $\sum_{j \in ramp} P_{j,T-1}^u$ is the overall platoon size or total flow of vehicles discharged from the upstream intersection to the freeway on-ramp during the last cycle, $N_{j,T-2}^r$ is the number of vehicles in residual queue from the cycle before the last cycle, and RM_{T-1}^r is the ramp meter rate used in the last cycle.

The ramp meter rate is an input rather than a decision variable, thus the green times that are assigned to the phases that discharge traffic from the arterials to the freeway on-ramps must be reduced and assigned to the conflicting phases in order to reduce total delay. The total reduction in delay at the ramp meter and in the conflicting directions of the arterial traffic would outweigh the additional delay imposed on the on-ramp traffic due to limiting its corresponding green time at the signalized intersection upstream, thereby reducing the overall delay and preventing on-ramp queue spillbacks and queue overrides.

However, this new control strategy requires solving mix-integer linear programming (MILP) every cycle in order to determine which of the above cases apply, which can be difficult in real world implementation. Furthermore, this approach still assumes fixed cycle length, similar to the previous control strategy, and does not address the importance of selecting the appropriate cycle length to avoid queue spillback when the freeway on-ramp has queue storage constraints. Lastly, this approach intended to provide signal progression, which is not appropriate when there is queue storage constraint downstream.

4.3 Control Strategy III: Queue Length Minimization

A simple and readily implementable control strategy is presented to resolve the inefficient control of freeway ramp metering and arterial traffic signals, which fail to recognize oversaturation of metered on-ramps by using long cycle lengths and providing progression to the heavier direction, as well as activating queue override. The control strategy is intended to manage the on-ramp queues at most freeway corridors with metered on-ramps and adjacent arterials primarily used to facilitate freeway access.

Freeway Ramp Metering

The proposed control strategy for coordinating arterial traffic signals and freeway ramp metering is not limited to any specific freeway ramp metering algorithm. As a result, the ramp metering algorithm does not have to be modified, except for the queue override function that releases on-ramp queues onto the freeway to prevent spillback.

Under the more efficient arterial signal control intended to prevent queue spillback and mitigate unnecessary penalties, the freeway ramp meter no longer needs queue override because the arterial traffic signals can now compensate for the negative impact of on-ramp queues on nearby arterials as a result of metering freeway on-ramps restrictively. This would mitigate the capacity drop as a result of releasing on-ramp queue on the freeway.

Arterial Traffic Signals

There have been numerous proposed mathematical models for estimating delay at signalized intersections. The most commonly used approach is the approximate steady state expression of delay proposed by Webster. The delay of each phase or turning movement at a signalized intersection is the following:

$$d = \frac{c[1 - (g/C)]^2}{2[1 - (g/C)x]} + \frac{x^2}{2v(1 - x)} - 0.65\left(\frac{C}{v^2}\right)^{\frac{1}{2}} x^{2+5(g/C)} \tag{4.17}$$

where,

d: average delay per vehicle (sec)
C: cycle length (sec)
g: effective cycle length (sec)
x: degree of saturation (sec)
v: arrival rate (veh/sec)

The first two terms correspond to the delay modelled using an *M/D/1* queuing system, which has Poisson arrival, deterministic service time, and single server. The last term corresponds to a correction term calibrated based on field data, in order to better reflect the real world conditions.

Furthermore, the effective green can be expressed as the following:

$$g = \frac{y}{Y} \cdot (C - L) \tag{4.18}$$

where,

y: ratio of arrival rate and saturation flow
Y: sum of y's of the cycle
L: total lost time (sec)

Substitute Equation 4.18 into Equation 4.17, the delay can expressed as a function of cycle length. An optimization model that minimizes the overall delay of the signalized intersection can be formulated to determine the optimal cycle length C_o:

$$C = \frac{1.5L + 5}{1 - Y} \tag{4.19}$$

Given the optimal cycle length, the corresponding effective green times can be determined using Equation 4.19. Additionally, offsets can be tuned to provide progression to the heavier direction if the signal timing plan is developed for an arterial corridor. Such approach has been widely used by the local transportation agencies and has been incorporated into commercial software for developing signal timing plans. Despite the popularity, this approach does not provide efficient signal timing plans for arterial intersections adjacent to saturated on-ramps with queue storage constraints.

During peak hours, the freeway ramp meter restricts the flow of the on-ramp in order to prevent capacity drop on the freeway. This limits the capacity of the on-ramp, and with the higher demand for on-ramp access from the adjacent arterial, excess accumulation can be observed at the on-ramp and eventually propagates to the arterial intersection. However, arterial traffic signals and freeway ramp meters currently operate independent of each other. The arterial traffic signal timing plans developed using method such as those outlined in Equation 4.17 to 4.19 do not consider the freeway on-ramp downstream and are developed under the assumption that the arterials do not have queue storage constraints. As a result, for relatively high demand during the peak hours, the optimal cycle length is relatively long in order to maximize capacity and reduce start-up lost time. Thus, long green times are given to the movements that feed the freeway on-ramp, and portions of the green times cannot be effectively utilized due to on-ramp queue storage space filling up before the green duration terminates. This causes vehicles to block the intersection and imposes unnecessary delay on the conflicting movements. Furthermore, due to the long green duration, the overflow of vehicles feeding the on-ramp activates queue override, which releases vehicles from the on-ramp to the freeway in order to mitigate queue spillback at the on-ramp. Unfortunately, activating queue override introduces more merging traffic to the freeway mainline, which triggers more lane changes and speed reduction in the median lane, and can result in capacity drop on the freeway.

Instead, the signalized arterial intersections near the freeway on-ramps are similar to a series of adjacent signalized intersection in over-saturated conditions. Thus, the signal timing plans for arterials adjacent to freeway on-ramps should be developed similar to signal timings of over-saturated arterials. Therefore, long cycle lengths and long green durations are not feasible; cycle lengths and green durations should consider the on-ramp queue storage space and should be designed to avoid queue spillback [17].

To illustrate the improved signal timing approach, consider a signalized intersection with 4 phases. In most real world cases, not every phase serves the turning movements that have on-ramp access. Thus, in this example, consider phase 1 and phase 2 as the turning movements feeding the on-ramp, and the remaining phases do not have on-ramp access.
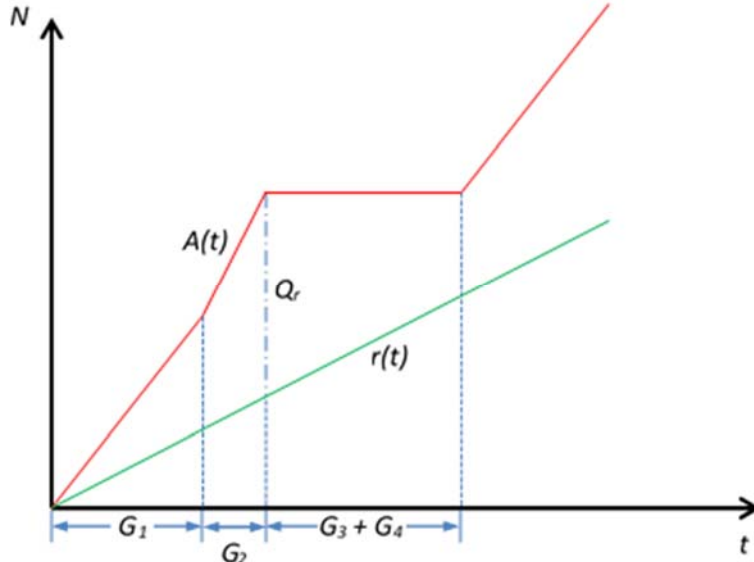
Figure 4.11: Queueing Diagram of Freeway On-ramp during a Signal Cycle

The queuing diagram in Figure 4.11 illustrates the upstream arrival patterns, downstream departure rate, and the excess accumulation of the freeway on-ramp when ramp metering is active and the demand from the upstream arterial exceeds the capacity of the metered on-ramp. Based on the queuing diagram, when the freeway on-ramp is metered at rate *r(t)*, the high arrival rate from phase 1 of the upstream signalized intersection results in excess accumulation on the on-ramp. Similarly, the excess accumulation grows after phase 2 begins. Since the arrival rates from both phase 1 and phase 2 are higher than the ramp meter rate, the green time for phase 1 and phase 2 must terminate at or before the excess accumulation reaches the maximum on-ramp queue storage capacity Q_r. The subsequent phases, which do not feed the on-ramp, can be served earlier, and when the subsequent phases terminate, a portion of the on-ramp will be available for storing the excess accumulation from phase 1 and phase 2 in the next cycle. This results in a relatively shorter cycle length. If longer cycle lengths were used thus the green times for phase 1 and phase 2 were terminated after the excess accumulation reaches the maximum on-ramp queue storage capacity, the arrival curve *A(t)* afterwards must be parallel to the departure curve with slope *r(t)*, the ramp meter rate. This is because the queue storage capacity of the on-ramp cannot be exceeded, thus the queue must be stored at the upstream arterial. In other words, if long green durations were provided to phase 1 and phase 2, vehicles from phase 1 and phase 2 would discharge at rates lower than the saturation flow rate for some portion of the cycle, which lead to lower capacity of the intersection. This can also impose unnecessary delay in the conflicting directions. The mathematical expressions for this concept of signal control are described in the next few paragraphs.

First, the excess accumulation of the on-ramp must be estimated. Using the ramp meter rate $r(t)$ that is updated each time step *t*, the on-ramp excess accumulation at time step *t* can be determined based on the following process:

$$Q(0) = 0$$

$$Q(1) = Q(0) + A(1) - D(1)$$

$$Q(2) = Q(1) + A(2) - D(2)$$

$$\vdots$$

$$Q(t) = Q(t-1) + A(t) - D(t)$$

39

$Q(t)$ is the on-ramp excess accumulation at the end of time step t, $A(t)$ is the number of arrivals from upstream of the on-ramp during time step t, and $D(t)$ is the number of departures from ramp meter during time step t. The arrivals and departures can be measured by the loop detectors at the upstream and downstream ends of the freeway on-ramp, respectively. The on-ramp excess accumulation should be updated at the end of every cycle in order to perform real time control.

Equation 4.20 is developed using the queuing diagram in Figure 4.11, to ensure that the green time for phase 1 and phase 2 must terminate at or before the excess accumulation reaches the maximum on-ramp queue storage capacity Q_r, therefore imposes an upper limit for the cycle length:

$$Q(t-1) + g_1 \cdot s_1 \cdot \beta_1 + g_2 \cdot s_2 \cdot \beta_2 - g_1 \cdot r(t) - g_2 \cdot r(t) - 2l \cdot r(t) \leq Q_r \qquad (4.20)$$

where,

g_1: effective green time of phase 1
g_2: effective green time of phase 2
s_1: saturation flow of phase 1
s_2: saturation flow of phase 2
β_1: percentage of demand of phase 1 that access the on-ramp
β_2: percentage of demand of phase 2 that access the on-ramp
$Q(t-1)$: residual on-ramp queue from the previous cycle.
$r(t)$: ramp metering rate
l: lost time of each phase (sec)

Similar to Equation 4.18, the effective green times can be expressed as functions of cycle length. Thus, g_1 and g_2 are expressed as the following:

$$g_1 = \frac{y_1}{Y} \cdot (C - 4l) \qquad (4.21)$$

$$g_2 = \frac{y_2}{Y} \cdot (C - 4l) \qquad (4.22)$$

where,

y_1: ratio of arrival rate and saturation flow of phase 1
y_2: ratio of arrival rate and saturation flow of phase 2
Y: sum of y's of the cycle
C: cycle length (sec)

Substitute Equations 4.21 and 4.22 into equation 4.20, equation 4.20 can be expressed in terms of cycle length. Solving for cycle length in terms of the rest of the variables, the upper limit of cycle length is the following:

$$C \leq \frac{[Q_r - Q(t-1) + r(t) \cdot 2l] \cdot Y + 4l \cdot \left[\sum_{i=1,2} s_i \beta_i y_i - \sum_{i=1,2} r(t) y_i\right]}{\left[\sum_{i=1,2} s_i \beta_i y_i - \sum_{i=1,2} r(t) y_i\right]} \qquad (4.23)$$

The upper limit of the cycle length must be updated at the end of every cycle in order to perform real time control that coordinates with freeway ramp metering.

If the on-ramp has sufficient queue storage space, the upper limit of the cycle length is typically higher than the optimal cycle length determined using Webster's formula or other similar methods, thus in this case,

the cycle length remains unchanged. On the other hand, when there is limited on-ramp queue storage, the upper limit of the cycle length is typically lower than the optimal cycle length determined using Webster's formula or other similar methods, and in this case, the upper limit takes precedence in order to reduce the cycle length and prevent queue spillback at the on-ramp and its nearby arterial intersections. With the new cycle length, the effective green times are still determined using Equation 4.18.

Additionally, many signalized intersection are timed using the dual ring structure. A typical example shown in Figure 4.12 is a four-leg signalized intersection with 8 phases, and each phase represents a turning movement. Phases 1 and 3 correspond to the leading left turns while phases 6 and 8 correspond to the lagging left turns, and the rest of the phases represent the through movements. There is a center barrier to prevent conflicts among turning movement of the north-south and the east-west directions.

1	2	3	4
5	6	7	8

Figure 4.12: Typical Dual Ring Structure of a Four-leg Intersection

As an example, phase 1 and phase 2 correspond to the turning movements feeding the on-ramp. Similarly, Figure 4.13 illustrates the upstream arrival patterns, downstream departure rate, and the excess accumulation of the freeway on-ramp when ramp metering is active and the demand from the upstream arterial exceeds the capacity of the metered on-ramp. The methodology for determining the upper limit of the cycle length is the same as before, with the exception of how the effective green times are computed.
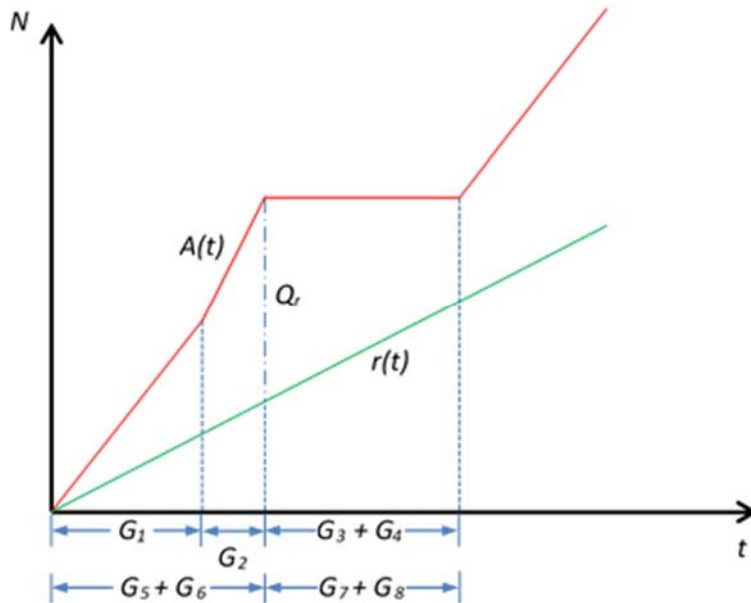
Figure 4.13: Queueing Diagram of Freeway On-ramp during a Signal Cycle (Dual Ring)

To formulate the expression for the effective green times, let y_L denote the ratio of arrival rate and saturation flow of all phases to the left of the barrier, similarly, let y_R denote the ratio of arrival rate and saturation flow of all phases to the right of the barrier. They are defined as the following:

$$y_L = \max(y_1 + y_2, y_5 + y_6) \tag{4.24}$$

$$y_R = \max(y_3 + y_4, y_7 + y_8) \tag{4.25}$$

Where y_i denotes the ratio of arrival rate and saturation flow of phase i, for $i = 1,2,\ldots,7,8$.

Then, the effective green times for phase 1 and phase 2 are defined as the following:

$$g_1 = \frac{y_1}{y_1 + y_2} \cdot \frac{y_L}{y_L + y_R} \cdot (C - 4l) \tag{4.26}$$

$$g_2 = \frac{y_2}{y_1 + y_2} \cdot \frac{y_L}{y_L + y_R} \cdot (C - 4l) \tag{4.27}$$

For the remaining phases, the effective green times are:

$$g_3 = \frac{y_3}{y_3 + y_4} \cdot \frac{y_R}{y_L + y_R} \cdot (C - 4l) \tag{4.28}$$

$$g_4 = \frac{y_4}{y_3 + y_4} \cdot \frac{y_R}{y_L + y_R} \cdot (C - 4l) \tag{4.29}$$

$$g_5 = \frac{y_5}{y_5 + y_6} \cdot \frac{y_L}{y_L + y_R} \cdot (C - 4l) \tag{4.30}$$

$$g_6 = \frac{y_6}{y_5 + y_6} \cdot \frac{y_L}{y_L + y_R} \cdot (C - 4l) \tag{4.31}$$

$$g_7 = \frac{y_7}{y_7 + y_8} \cdot \frac{y_R}{y_L + y_R} \cdot (C - 4l) \tag{4.32}$$

$$g_8 = \frac{y_8}{y_7 + y_8} \cdot \frac{y_R}{y_L + y_R} \cdot (C - 4l) \tag{4.33}$$

Substitute Equations 4.26 and 4.27 into Equation 4.20, Equation 4.20 can be expressed in terms of cycle length. Solving for cycle length in terms of the rest of the variables, the upper limit of cycle length is the following:

$$C \leq \frac{[Q_r - Q(t-1) + r(t) \cdot 2l] \cdot (y_L + y_R)}{\left[\frac{(s_1 \cdot \beta_1 - r(t)) \cdot y_1 y_L}{y_1 + y_2} + \frac{(s_2 \cdot \beta_2 - r(t)) \cdot y_2 y_L}{y_1 + y_2}\right]} \tag{4.34}$$

If phase 2 and phase 3, instead of phase 1 and phase 2, correspond to the turning movements feeding the on-ramp, then the upper limit of the cycle length becomes:

$$C \leq \frac{[Q_r - Q(t-1) + r(t) \cdot 2l] \cdot (y_L + y_R)}{\left[\frac{(s_2 \cdot \beta_2 - r(t)) \cdot y_2 y_L}{y_1 + y_2} + \frac{(s_3 \cdot \beta_3 - r(t)) \cdot y_2 y_L}{y_3 + y_4}\right]} \tag{4.35}$$

Similar to previous discussions, the upper limit of the cycle length must be updated at the end of every cycle in order to perform real time control that coordinates with freeway ramp metering. The effective green times can be computed using Equations 4.26 through 4.33.

Lastly, adjacent arterial signals should not be coordinated to ensure uninterrupted flow and progression because every major intersection is a capacity-constrained due to the on-ramp nearby. Thus, coordination of adjacent signals should also be done similar to the coordination of oversaturated signals. There should

be simultaneous offset (zero offset) when it is congested downstream of the major intersection with access to the freeway on-ramp. This would allow the residual queue at the downstream intersection to dissipate in time, otherwise, large platoons of vehicles would arrive from upstream intersection before the downstream residual queues are served, which can fill up the limited queue storage space and cause spillback upstream. Furthermore, most users of the arterials adjacent to the freeways travel a short segment to access the nearest freeway on-ramp rather than a long segment of the arterial, thus progression for a long stretch of arterial is not appropriate. In such case, each signalized intersection should be timed independently to avoid assigning the longest cycle length to all of the signalized intersections, which can impose heavy delays to the conflicting directions and cause queue spillback when queue storage is constrained downstream.

Overall, the above approaches are intended to prevent queue spillback at the on-ramp and further upstream at the arterial, in order to mitigate any unnecessary penalty imposed on the conflicting directions of the arterial traffic and eliminate the need for queue override at the metered on-ramps.

4.4 Recommend Control Strategy

The control Strategy III (queue length minimization) was selected as the control strategy for coordinating freeway ramp metering and arterial traffic signals due to its simplicity and feasibility for real world implementation. This approach requires minimal real time detection; it only needs the arrival and departure flows at the upstream and downstream ends of the on-ramp, and they can be measured using the existing inductive loop detectors. Other than the on-ramp detection, this coordination scheme only requires real time modifications of the signal controller and ramp metering settings. For ramp metering, the queue override function must be disabled. For arterial traffic signals, cycle lengths and green times are modified at the end of every cycle.

Overall, coordination of freeway ramp metering and arterial traffic signal does not require any new surveillance technologies or infrastructural changes and can be accomplished using the existing infrastructure and detection capabilities, thus can be implemented with minimal cost. Additionally, it addresses the importance of selecting the appropriate cycle length when queue storage downstream of the signalized intersection is constrained.

CHAPTER 5

EVALUATION OF PROPOSED STRATEGIES

5.1 Simulation Model Development

In order to evaluate the proposed control strategy for coordinating freeway ramp metering and arterial traffic signals, a microscopic simulation model was built in the AIMSUN microscopic simulation model [18] using the most up to date road geometry, lane configurations, and speed limits of the freeway and the arterial at the selected site. The simulation model covered four miles of northbound I-680, the on-ramps and off-ramps at Alum Rock Ave., McKee Rd., and Berryessa Rd., the parallel arterial Capitol Ave., and 15 signalized intersections. Freeway and arterial data obtained from the morning peak (7:00 AM to 9:30 AM) of September 23, 2015 were used for the inputs in demand and turning percentages. During the morning peak of September 23, 2015, freeway ramp meters and arterial traffic signals were functioning properly and there were no incidents within the selected corridor.

For the freeway, 5-minute interval loop detector data for flow were obtained from PeMS [19] and used as the demand input at the most upstream location of the simulation network and as the turning percentages at any applicable mainline-off-ramp split. Ramp metering rates and algorithms were obtained from Caltrans District 4 and modeled in microscopic simulation via AIMSUN API (Application Programming Interface). Ramp metering has been active since September 1, 2015.

For the arterial, video cameras were placed at the signalized intersections and arterial-on-ramp splits during the morning peak of September 23, 2015. Turning movement flows were recorded every 5 minutes, and they were used as the demand input at the entry points of the corridor (i.e. Southbound Capitol north of Berrryessa Rd.) and as turning percentages at the signalized intersections and the arterial-on-ramp splits. The signal timing plans for the coordinated actuated signals were provided by the city of San Jose.

The model was calibrated to existing conditions prior to the evaluation of the proposed control strategy. Twenty replications of the simulation model runs with different random number seeds were made using the existing demand, turning percentages, ramp metering algorithm, and signal timing plans. The predicted flows and speeds at selected locations on the freeway mainline were compared with real traffic measurements in every 5 minutes to assess the accuracy of the simulation model in representing observed conditions. For flows, we need at least 85% of the flows to be acceptable and GEH<5 [20]. According to this criterion, the predicted flow is acceptable if it satisfies the requirement below.

Link flow quantity
- If 700 vph < real flow < 2700 vph, simulated flow has an error within 15%;
- If real flow < 700 vph, simulated flow has an error within 100 vph;
- If real flow > 2700 vph, simulated flow has an error within 400 vph.

The GEH statistic is computed as

$$GEH(k) = \sqrt{\frac{2[M(k) - C(k)]^2}{M(k) + C(k)}} \qquad (5.1)$$

Where:

$M(k)$: simulated flow during the k-th time interval (veh/hour)
$C(k)$: flow measured in the field during the k-th time interval (veh/hour)

A satisfactory calibration requires that on average of all detectors, for at least 85% of all 5-minute time intervals, the flow is to satisfy the condition $GEH(k) < 5$. For speed, the relative root mean squared error

(RRMSE) of simulated speed values are required to be 15% or lower, on average of all detectors. For arterial flows, GEH < 5 must be satisfied for at least 85% of all 5-minute time intervals, for each turning movement of the major intersections.

Tables 5.1 and 5.2 summarize the calibration results for the three detectors along the four mile stretch of Northbound I-680, as well as the 5-minute turning movement flows of the major arterial intersections. Figures 5.1 through 5.3 compare the speed data collected from the field with the simulated data. It can be seen that on average, for the freeway, the simulated flows and speeds satisfy the calibration criteria. Similarly, the simulated flows at major arterial intersections satisfy the calibration criterion. Calibration was not performed in the southbound freeway direction because of the low volume during the morning peak analysis periods.

Table 5.1 Calibration of Freeway and Arterial Flows

Freeway: 5-min flows of I-680 Northbound					
Detector Location	Target	Cases	Cases Met	% Met	Target Met?
Alum Rock Ave. on-ramp (loop)	GEH < 5 for > 85% of k	24	24	100.00%	Yes
McKee Rd. on-ramp	GEH < 5 for > 85% of k	24	24	100.00%	Yes
Berryessa Rd. on-ramp	GEH < 5 for > 85% of k	24	23	95.83%	Yes
Overall	GEH < 5 for > 85% of k	72	71	98.61%	Yes
Arterial: 5-min flows of major intersections					
Capitol Ave. & Alum Rock Ave.					
	Target	Cases	Cases Met	% Met	Target Met?
Northbound	GEH < 5 for > 85% of k	48	47	97.92%	Yes
Southbound	GEH < 5 for > 85% of k	48	48	100.00%	Yes
Westbound	GEH < 5 for > 85% of k	48	48	100.00%	Yes
Eastbound	GEH < 5 for > 85% of k	48	48	100.00%	Yes
Capitol Ave. & Berryessa Rd.					
	Target	Cases	Cases Met	% Met	Target Met?
Northbound	GEH < 5 for > 85% of k	48	48	100.00%	Yes
Southbound	GEH < 5 for > 85% of k	72	72	100.00%	Yes
Westbound	GEH < 5 for > 85% of k	48	48	100.00%	Yes
Eastbound	GEH < 5 for > 85% of k	72	72	100.00%	Yes
Capitol Ave. & Mabury Rd.					
	Target	Cases	Cases Met	% Met	Target Met?
Northbound	GEH < 5 for > 85% of k	48	48	100.00%	Yes
Southbound	GEH < 5 for > 85% of k	48	48	100.00%	Yes
Westbound	GEH < 5 for > 85% of k	48	48	100.00%	Yes
Eastbound	GEH < 5 for > 85% of k	48	48	100.00%	Yes
Capitol Ave. & McKee Rd.					
	Target	Cases	Cases Met	% Met	Target Met?
Northbound	GEH < 5 for > 85% of k	48	46	95.83%	Yes
Southbound	GEH < 5 for > 85% of k	72	71	98.61%	Yes
Westbound	GEH < 5 for > 85% of k	48	48	100.00%	Yes
Eastbound	GEH < 5 for > 85% of k	72	70	97.22%	Yes
Alum Rock Ave. & I-680 Northbound Off-ramp					
	Target	Cases	Cases Met	% Met	Target Met?
Northbound	GEH < 5 for > 85% of k	48	48	100.00%	Yes
Westbound	GEH < 5 for > 85% of k	48	48	100.00%	Yes
Eastbound	GEH < 5 for > 85% of k	48	47	97.92%	Yes
Arterial: Overall	GEH < 5 for > 85% of k	1008	1001	99.30%	Yes

45

Table 5.2 Calibration of Freeway Speeds

	Detector Location		
	Alum Rock Ave. on-ramp (loop)	McKee Rd. on-ramp	Berryessa Rd. on-ramp
RMSSE	2.21%	16.14%	13.80%
Target	<15%	<15%	<15%
Target Met?	Yes	No	Yes
Overall	**10.72%**		
Target	**RMSSE<15%**		
Target Met?	**Yes**		
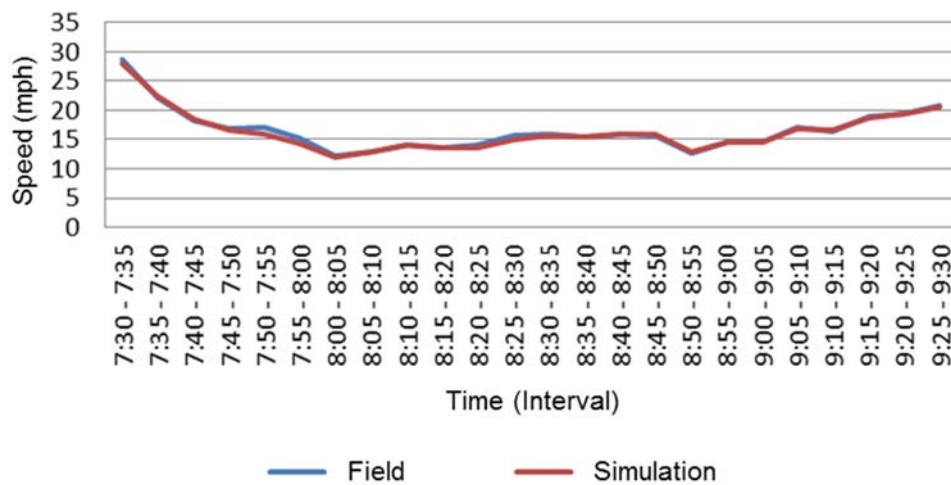
Figure 5.1 Observed and Simulated Speeds near Alum Rock Ave. On-ramp (loop)
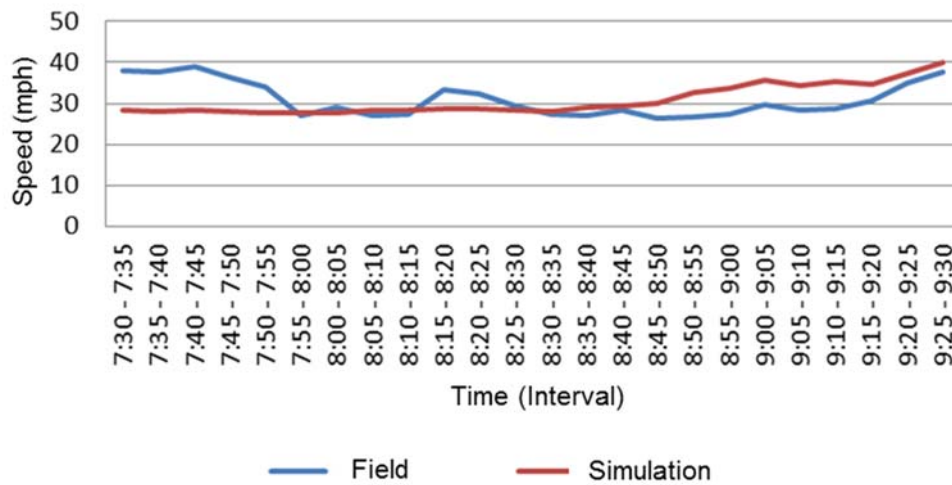
Figure 5.2 Observed and Simulated Speeds near McKee Rd. On-ramp
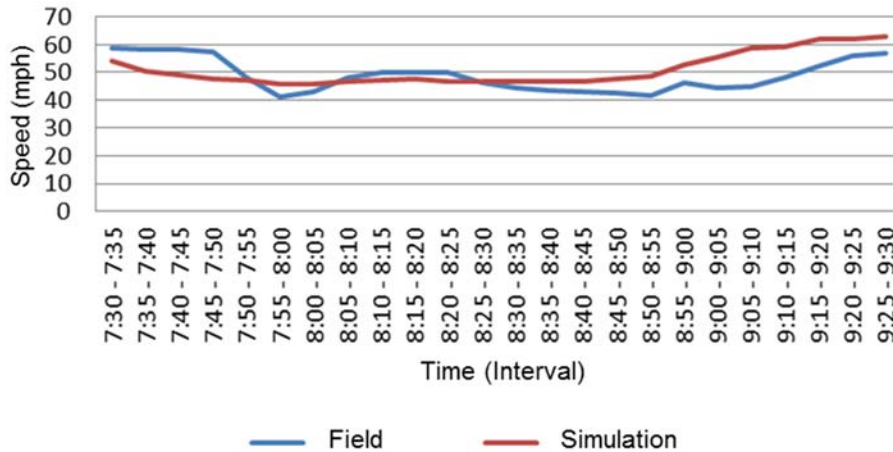
Figure 5.3 Observed and Simulated Speeds near Berryessa Rd. On-ramp

5.2 Testing of Proposed Control Strategies

Simulation tests were conducted to determine the effectiveness of the recommended control strategy III described in Chapter 4. First simulations were performed with the changes in the signal control only, in order to determine the benefit of only using the improved signal timing. Queue override was not disabled for this test. Next, experiments were conducted to determine the effect of queue override; simulations were run using the existing control with the ramp meter's queue override function activated and deactivated, and then repeated using the latest control strategy (for arterial signals) with the ramp meter's queue override function activated and deactivated. Twenty replications were run in each of the scenarios described above.

As shown in Table 5.3, when the proposed control for arterial traffic signals were implemented without any modifications to freeway ramp metering (with queue override staying active), the arterial performance improved. Delay reductions were observed in both direction of the parallel arterial Capitol Ave., due to more efficient signal timing that prevents long cycle length and on-ramp queue spillback at the intersections adjacent to the on-ramps. Furthermore, the benefit can be attributed to the simultaneous offset that allows residual queue at the downstream intersection to dissipate prior to the arrivals of vehicles from the upstream intersection. In addition, the reduced cycle lengths mitigated the long delays imposed on the cross streets. There were significant delay reductions at McKee Rd. and Berryessa Rd. but almost none at Alum Rock Ave. This is because there is sufficient space for on-ramp queue storage near the Alum Rock Ave. on-ramp thus queue spillback was not prevalent and the signal timing remained the same, on the other hand, queue storage space were limited at the McKee Rd. and Berryessa Rd. on-ramps therefore the cycle lengths were reduced at the corresponding signalized intersections, which reduced the penalty imposed on the cross streets. The reduction in delay is also shown in the improvement in level of service (LOS). Lastly, as expected, the freeway performance remained roughly the same, as shown in Table 5.3, and we can conclude that the proposed control for arterial traffic signals reduced system-wide delay by improving the arterial performance.

Further simulation experiments investigated the effect of queue override and the results are summarized in Tables 5.4 and 5.5. As shown in in Table 5.4, under the existing control of arterial traffic signals and freeway ramp metering, deactivating queue override did not improve the system-wide performance because the very small observed changes in total distance travelled and total delay were largely due to stochastic variation. Similarly, the observed change in total distance travelled on the freeway was mostly resulted from stochastic variation. However, there were significant delay reduction awarded to the freeway when queue override was deactivated. Therefore, deactivating queue override was not helpful to the overall system because it merely transferred the delay from the freeway to the arterial, contrary to the hypothesis that

47

deactivating queue override could mitigate capacity drop and increase system-wide throughput. Similar observations can be made for the case with the proposed control strategy for coordinating freeway ramp metering and arterial traffic signals, as shown in Table 5.5. Deactivating queue override was not helpful to the overall system because it redistributed the freeway and arterial delay.

5.3 Conclusion

In summary, the simulation results reveal that the proposed control provide more efficient signal timing and reduced the system-wide delay as a result. The benefit is given to the arterial but can be redistributed from the arterial to the freeway by deactivating the queue override function of freeway ramp metering. This provides two options to the jurisdictions operating the freeway ramp metering and arterial traffic signals; the first option is implementing the proposed control strategy with queue override activated and the results are shown in Table 5.3, the latter option is implementing the proposed control strategy with queue override deactivated and the results are shown in Table 5.6. However, if empirical evidence suggests queue override reduces freeway capacity, the latter option must be selected because deactivating queue override can bring additional benefit by increasing the freeway capacity.

Table 5.3 Performance of Proposed Control with Queue Override Activated

	Before Coordination		**After Coordination**		**% Difference**	
Arterial Performance						
Average Delay of Parallel Arterial (min/veh)						
Capitol Ave NB	8.63		8.26		-4.29%	
Capitol Ave SB	5.72		5.34		-6.65%	
Average Delay of Cross Street (sec/veh)						
Alum Rock WB	48.05 (D)*		48.22 (D)*		-1.74%	
Alum Rock EB	37.27 (D)*		37.34 (D)*		0.19%	
McKee WB	56.76 (E)*		32.73 (C)*		-42.34%	
McKee EB	28.92 (C)*		14.77 (B)*		-48.91%	
Berryessa WB	47.27 (D)*		31.23 (C)*		-34.41%	
Berryessa EB	50.50 (D)*		34.85 (C)*		-44.92%	
Freeway Performance						
	Total Delay (veh-hr)	Total Distance Traveled (veh-miles)	Total Delay (veh-hr)	Total Distance Traveled (veh-miles)	Change in Total Delay	Change in Total Distance Traveled
I-680 NB	399.53	18894.07	406.10	18896.87	1.65%	0.01%
Overall Performance						
Freeway & Arterial	2847.02	71167.11	2620.67	71168.48	-7.95%	0.00%

*(Level of Service)

Table 5.4 Effect of Queue Override on the Current Control

	Override		No Override			
Freeway Performance						
	Total Delay (veh-hr)	Total Distance Traveled (veh-miles)	Total Delay (veh-hr)	Total Distance Traveled (veh-miles)	Change in Total Delay	Change in Total Distance Traveled
I-680 NB	399.53	18894.07	329.62	18710.00	-17.50%	-0.97%
Overall Performance						
Freeway & Arterial	2847.02	71167.11	2891.79	70570.96	1.57%	-0.84%

Table 5.5 Effect of Queue Override on the Proposed Control

	Override		No Override			
Freeway Performance						
	Total Delay (veh-hr)	Total Distance Traveled (veh-miles)	Total Delay (veh-hr)	Total Distance Traveled (veh-miles)	Change in Total Delay	Change in Total Distance Traveled
I-680 NB	406.10	18896.87	327.91	18647.88	-19.26%	-1.32%
Overall Performance						
Freeway & Arterial	2620.67	71168.48	2642.36	70169.60	0.83%	-1.40%

Table 5.6 Performance of Proposed Control with Queue Override Activated

	Before Coordination		After Coordination		% Difference	
Arterial Performance						
Average Delay of Parallel Arterial (min/veh)						
Capitol Ave NB	8.63		10.51		21.84%	
Capitol Ave SB	5.72		5.91		3.33%	
Average Delay of Cross Street (sec/veh)						
Alum Rock WB	48.05 (D)*		47.33 (D)*		-1.43%	
Alum Rock EB	37.27 (D) *		37.82 (D)*		1.47%	
McKee WB	56.76 (E)*		52.34 (D)*		-7.79%	
McKee EB	28.92 (C)*		16.51 (B)*		-42.91%	
Berryessa WB	47.27 (D)*		39.26 (D)*		-16.73%	
Berryessa EB	50.50 (D)*		37.55 (D)*		-34.48%	
Freeway Performance						
	Total Delay (veh-hr)	Total Distance Traveled (veh-miles)	Total Delay (veh-hr)	Total Distance Traveled (veh-miles)	Change in Total Delay	Change in Total Distance Traveled
I-680 NB	399.53	18894.07	327.91	18647.88	-17.93%	1.30%
Overall Performance						
Freeway & Arterial	2847.02	71167.11	2642.36	70169.60	-7.19%	-1.40%

*(Level of Service)

CHAPTER 6

QUEUE OVERRIDE FIELD STUDY

As shown in the previous chapter, based on the microscopic simulation results, deactivating queue override does not increase freeway capacity. However, microscopic simulation relies on assumptions in driving behavior that may not represent the real world conditions, and cannot accurately model the freeway capacity drop observed when the freeway becomes congested. Therefore, a field study was conducted to determine whether deactivating queue override increases freeway capacity.

6.1 Methodology

Due to practical limitations and concerns for negative impact on arterial traffic, the ramp metering plan cannot be altered (for deactivating queue override) during the course of the field study. Thus, a before and after study of queue override deactivation cannot be conducted. Fortunately, historical records showed that queue override stay active for only a portion of the morning peak period, as a result, an observational study of the freeway bottleneck during periods with and without queue override at the metered on-ramp was planned and conducted.

In order to reduce complexity, the scope of the field study was limited to only one bottleneck. The bottleneck must be isolated from any other bottlenecks downstream in order to measure the bottleneck discharge rate. Thus, the Berryessa Rd. bottleneck was considered. However, careful analysis of detector data from PeMS [19] revealed this bottleneck is not always active. As a result, the nearby McKee Rd. bottleneck was selected because it is fairly isolated (about one mile apart) from the downstream bottleneck at Berryessa Rd. Figure 6.1 shows road geometry of the selected bottleneck. Video cameras were placed upstream and downstream of the McKee Rd. on-ramp merge during the study periods of May 9, 2016 to May 13, 2016 and May 16, 2016 to May 20, 2016, and the camera locations are shown in Figure 6.1. The camera placed upstream recorded all hour mainline lanes, as well as the on-ramp. Vehicle count of each location and each 30 second interval was extracted from the video data.
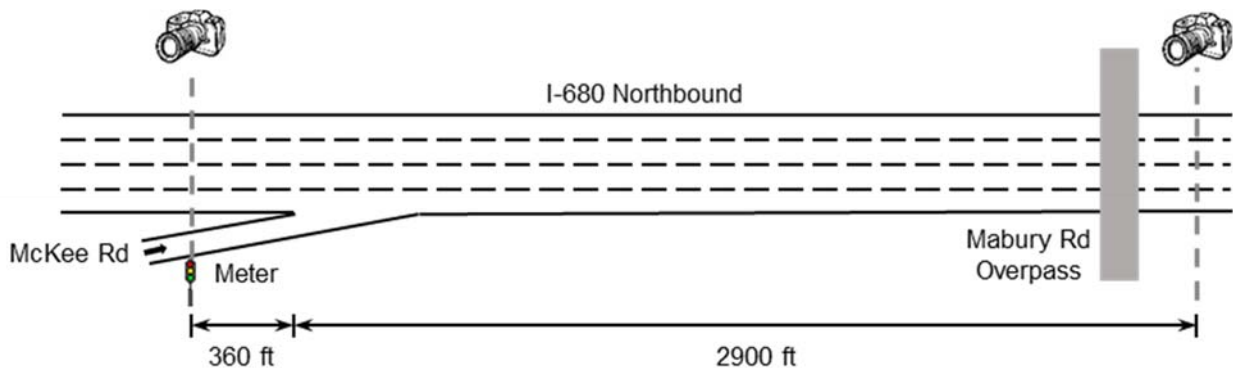
Figure 6.1 Queue Override Field Study Site

Figures 6.2 through 6.11 show the curves for cumulative vehicle count, obtained at the upstream and downstream locations, vs time, t. The curves were plotted to display virtual departures as a function of time at the downstream location. The vertical displacement between the curves is the excess accumulation on the freeway segment of interest due to the limited capacity, and the area between the curves indicate the total delay of the freeway system (mainline and on-ramp combined) [21].

The vertical scales in Figures 6.2 to 6.11 corresponds to cumulative count at the upstream and downstream locations shown in Figure 6.1 but were modified by plotting on the oblique coordinate system, in order to make the excess accumulation (vertical displacement) more noticeable. $O(t)$, the oblique coordinate transformation of the cumulative vehicle count, $V(t)$, is described by the following:

$$V(t) - q_0(t - t_0)$$

where,

q_0: specified reference value of flow
t_0: specified reference value of initial time

This coordination transformation also makes changes in the slope of the cumulative vehicle count curve, or flow, more noticeable by visual inspection. This approach has been widely used in recent works [22, 23, 24].

6.2 Field Study Results

The $O(t)$ curves shown in Figure 6.2 reveal that the demand did not exceed the capacity (both curves overlap) on Monday May 9, 2016. However, the outflow between $t = 7:30$ and $t = 7:50$ is fairly high at 8909 vph. Ramp metering remained active but queue override was not active during the morning peak period, due to insufficient on-ramp demand. Thus, the existing ramp metering plan maintained the high capacity.
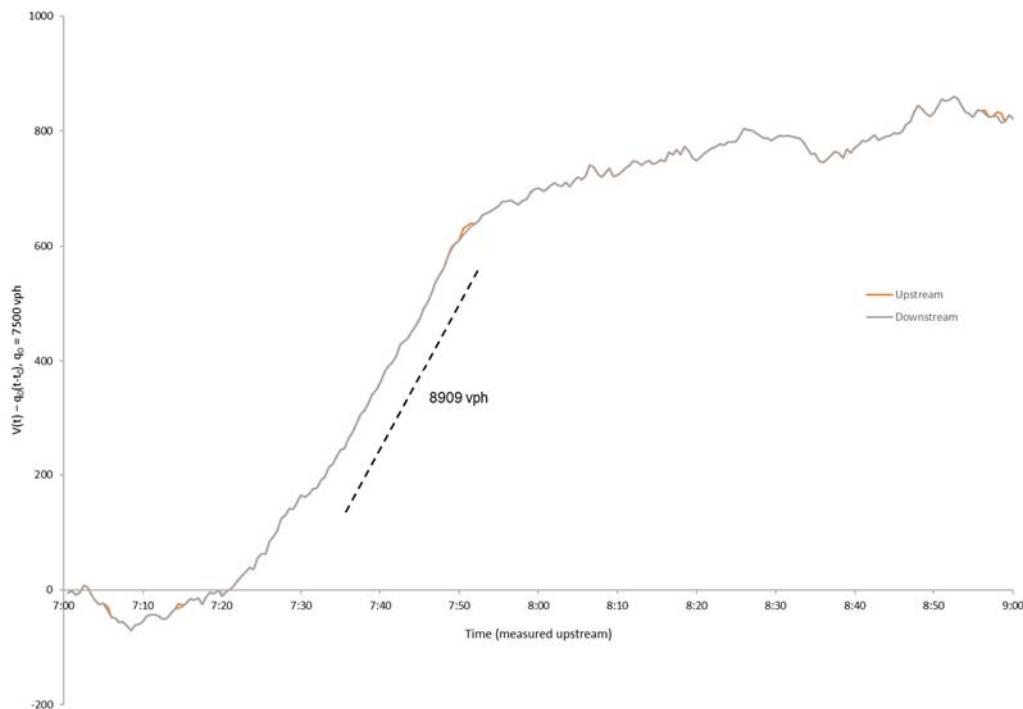
Figure 6.2 Cumulative Vehicle Counts (oblique scale) of May 9, 2016 (Monday)

Figure 6.3 shows the cumulative counts obtained from Tuesday May 10, 2016, which represents a typical morning peak period. From the $O(t)$ curves, it can be observed that shortly after $t = 7:10$, the outflow of the freeway bottleneck significantly increased due to the rise in the morning peak demand. However, both $O(t)$ curves roughly overlapped despite the higher demand at the beginning of the morning peak. These

observations indicate that traffic is free-flowing on the freeway mainline and on the section of the on-ramp downstream of the ramp meter. The observed condition persisted until $t = 7:33$, and the observed capacity is 8715 vph, as indicated by the left hand side dotted line.

At $t = 7:33$, there is sufficient on-ramp queue spillback to activate queue override, as a result, the ramp metering rate became less restrictive and remained at a maximum rate of 900 vph/lane. Queue override persisted until $t = 8:03:30$. As indicated by the dotted line on the right hand side of Figure 6.3, the outflow of the freeway bottleneck decreased to 8326 vph throughout the period of queue override activation, which translates to a 4.46% reduction in the bottleneck capacity.

The reduction in outflow was not a result of exogenous downstream bottleneck, after verifying, via loop detector data from PeMS [19], that free-flow condition was observed around Berryessa Rd. on-ramp downstream during the entire morning peak period. In addition to confirming that the bottleneck was isolated, Figure 6.3 shows that the demand did not reduce after queue override activated at $t = 7:33$, in fact, the $O(t)$ curves no longer overlap during the period in which queue override was activated. Thus, the less restrict metering rate as a result of queue override activation caused the reduced outflow. This phenomenon is called capacity drop and it has been empirically verified by the study in [24], but only for unrestricted merge rather than for metered on-ramps with queue override.

Once queue override terminated at $t = 8:03:30$, the freeway bottleneck returned to free-flow condition despite the persistence of high demand, as indicated by the overlapping $O(t)$ curves in Figure 6.3. Afterwards, the demand reduced and the $O(t)$ roughly overlapped until the end of the morning peak period at $t = 9:00$.
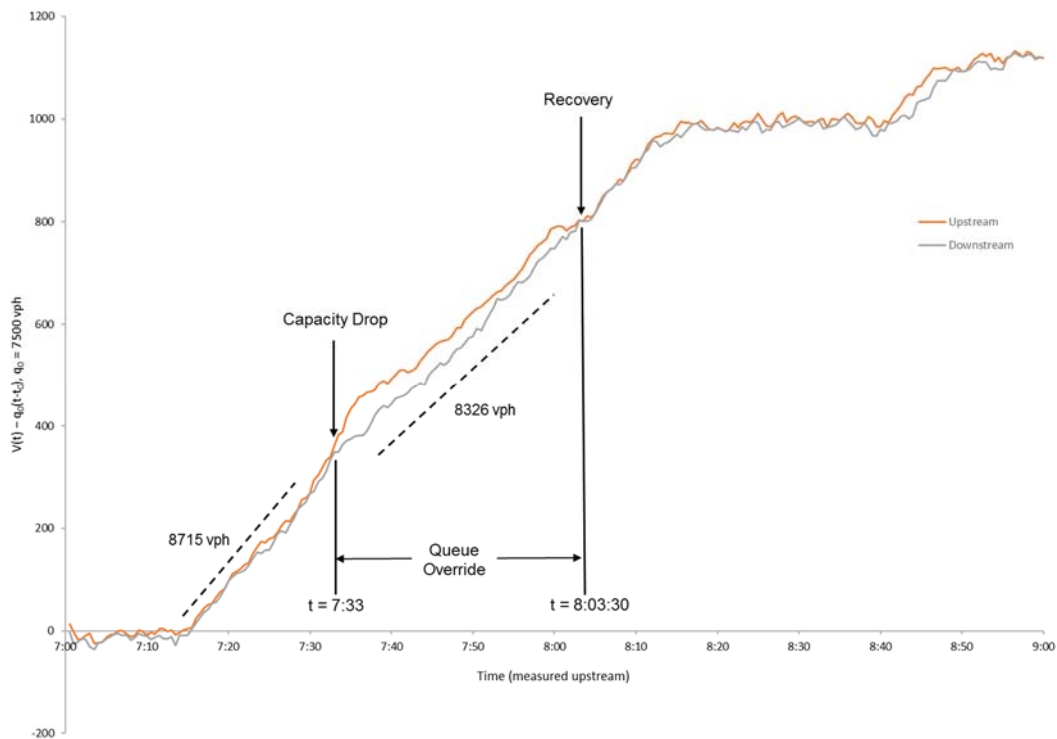
Figure 6.3 Cumulative Vehicle Counts (oblique scale) of May 10, 2016 (Tuesday)

Figure 6.4 shows the cumulative counts obtained from Wednesday May 11, 2016. From the $O(t)$ curves, it can be observed that at the beginning of the morning peak, the outflow of the freeway bottleneck remained fairly high in order to accommodate the peak period demand. The $O(t)$ curves mostly overlapped, except for a brief period of rapid demand increase around $t = 7:13$. These observed conditions continued until $t = 7:19$, and the observed capacity is 7958 vph, as indicated by the left hand side dotted line.

At $t = 7:19$, there is sufficient on-ramp queue spillback to activate queue override, and queue override was effective up to $t = 7:56$. During the time when queue override remained active, the outflow of the freeway bottleneck reduced to 7563 vph, indicted by the right hand side dotted line. Similar to the observations from May 10, 2016, the freeway bottleneck capacity reduced by 5.22%.

The reduction in outflow was not a result of exogenous downstream bottleneck, after verifying that free-flow condition persisted at Berryessa Rd. throughout the morning peak period. In addition to confirming that the bottleneck was isolated, Figure 6.4 shows that the demand did not reduce after queue override activated at $t = 7:19$. Once queue override terminated at $t = 7:56$, the freeway bottleneck began recovering from the capacity reduction and returned to free-flow condition after $t = 8:10$ despite the equally high demand. This is indicated by the overlapping $O(t)$ curves during the remainder of the morning peak period. Thus, queue override was the cause of the observed capacity drop.
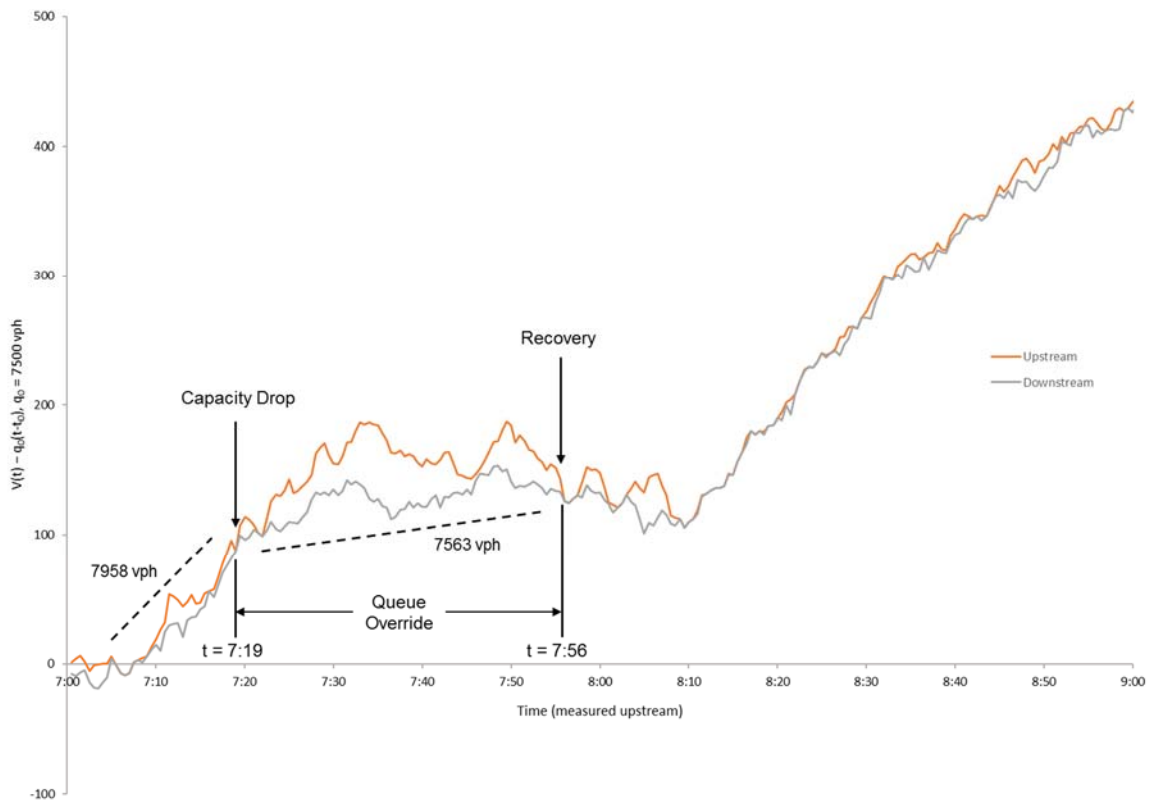
Figure 6.4 Cumulative Vehicle Counts (oblique scale) of May 11, 2016 (Wednesday)

Figure 6.5 shows the cumulative counts obtained from Thursday May 12, 2016. From the $O(t)$ curves, it can be observed that at $t = 7:15$ and shortly after, the outflow of the freeway bottleneck remained fairly high in order to accommodate the peak period demand. The $O(t)$ curves overlapped, which indicates that

traffic is free-flowing on the freeway mainline and on the section of the on-ramp downstream of the ramp meter. These observed conditions continued until $t = 7\!:\!34$, and the observed capacity is 9054 vph, as indicated by the left hand side dotted line.

At $t = 7\!:\!34$, there is sufficient on-ramp queue spillback to activate queue override, and queue override was effective up to $t = 8\!:\!04$. During the time when queue override remained active, the outflow of the freeway bottleneck reduced to 8176 vph, indicted by the right hand side dotted line. This translates to a 9.70% reduction in capacity.

The reduction in outflow was not a result of exogenous downstream bottleneck, after verifying that free-flow condition persisted at Berryessa Rd. throughout the morning peak period. In addition to confirming that the bottleneck was isolated, Figure 6.5 shows that the demand did not reduce after queue override activated at $t = 7\!:\!34$. Once queue override terminated at $t = 8\!:\!04$, the freeway bottleneck began recovering from the capacity reduction and returned to free-flow condition shortly after, despite the persistent high demand. This is shown by the overlapping $O(t)$ curves during the remainder of the morning peak period. Therefore, the observed capacity drop was a result of queue override.
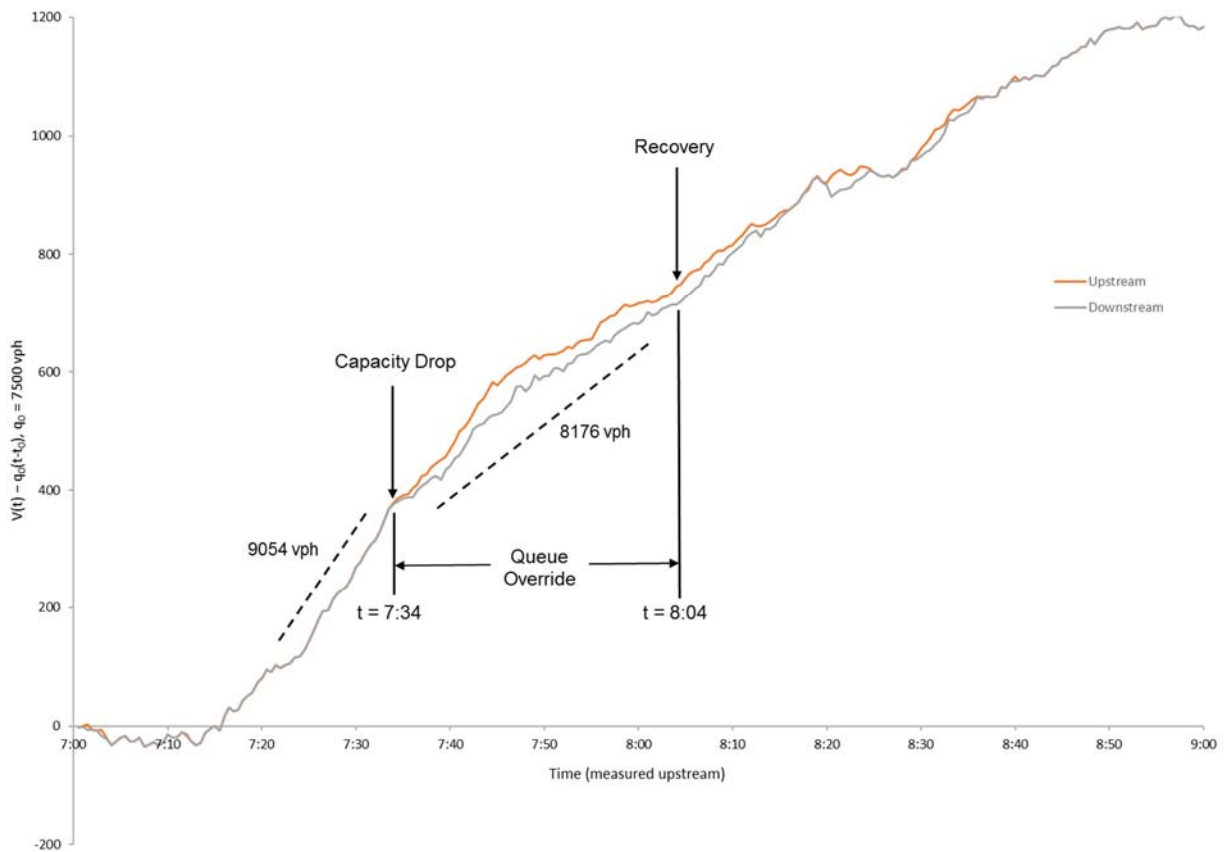
Figure 6.5 Cumulative Vehicle Counts (oblique scale) of May 12, 2016 (Thursday)

The $O(t)$ curves shown in Figure 6.6 reveal that the demand did not exceed capacity (both curves overlap and negative slope) on Friday May 13, 2016. This is due to the relatively lower demand at the end of the week.
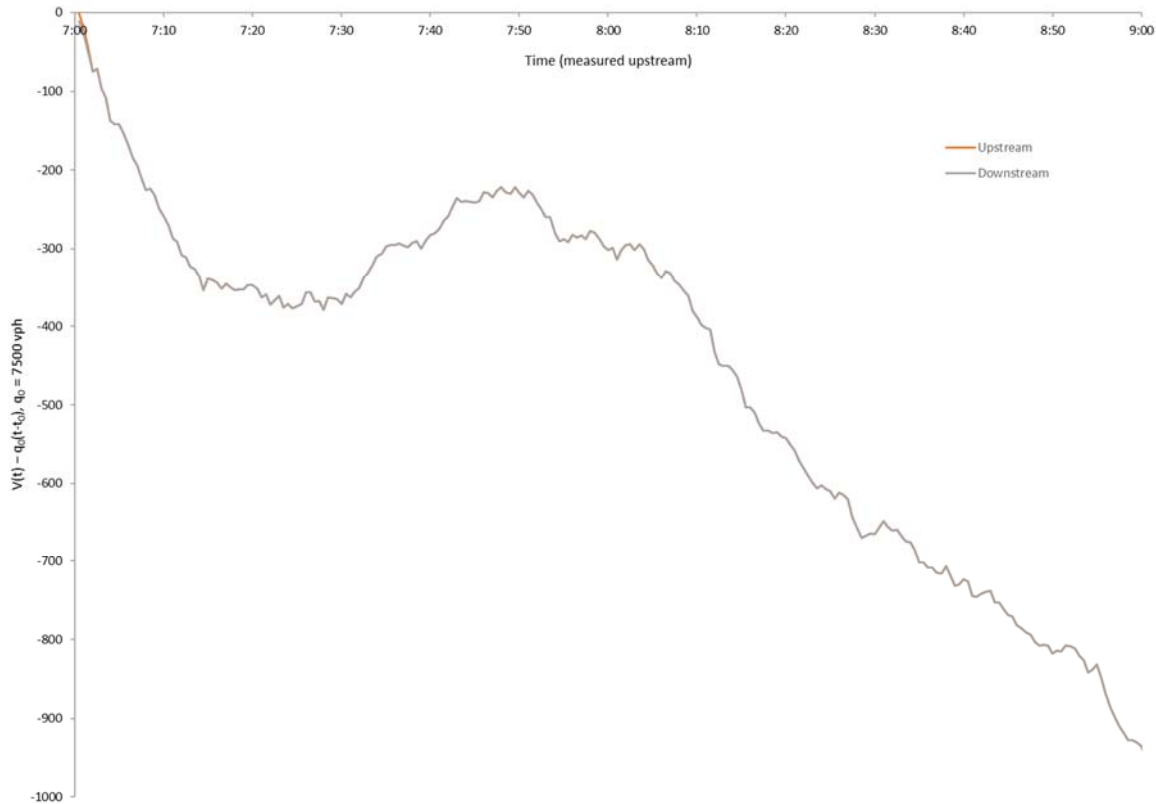
Figure 6.6 Cumulative Vehicle Counts (oblique scale) of May 13, 2016 (Friday)

Figure 6.7 shows the cumulative counts obtained from Monday May 16, 2016. From the $O(t)$ curves, it can be observed that at $t = 7{:}10$ and shortly after, the outflow of the freeway bottleneck remained fairly high in order to accommodate the peak period demand. The $O(t)$ curves overlapped, which indicates that traffic is free-flowing on the freeway mainline and on the section of the on-ramp downstream of the ramp meter. For the brief period before $t = 7{:}30$, the $O(t)$ curves no longer overlap due to the higher demand, nevertheless, the outflow remained relatively unchanged. The observed capacity is 9262 vph prior to $t = 7{:}30$, as indicated by the left hand side dotted line.

At $t = 7{:}30$, there is sufficient on-ramp queue spillback to activate queue override, and queue override was effective up to $t = 8{:}00$. During the time when queue override remained active, the outflow of the freeway bottleneck reduced to 8412 vph, as shown by the right hand side dotted line. This translates to a 9.18% reduction in capacity.

The reduction in outflow was not a result of exogenous downstream bottleneck, after verifying that free-flow condition persisted at Berryessa Rd. until $t = 8{:}03$. In addition to confirming that the bottleneck was isolated, Figure 6.5 shows that the demand did not reduce after queue override activated at $t = 7{:}34$. Data for times beyond $t = 8{:}03$ were not analyzed due to the fact that the exogenous downstream bottleneck was active from $t = 8{:}03$ to the end of the morning peak period. Regardless, there is sufficient evidence showing that queue override resulted in the observed capacity drop.

55
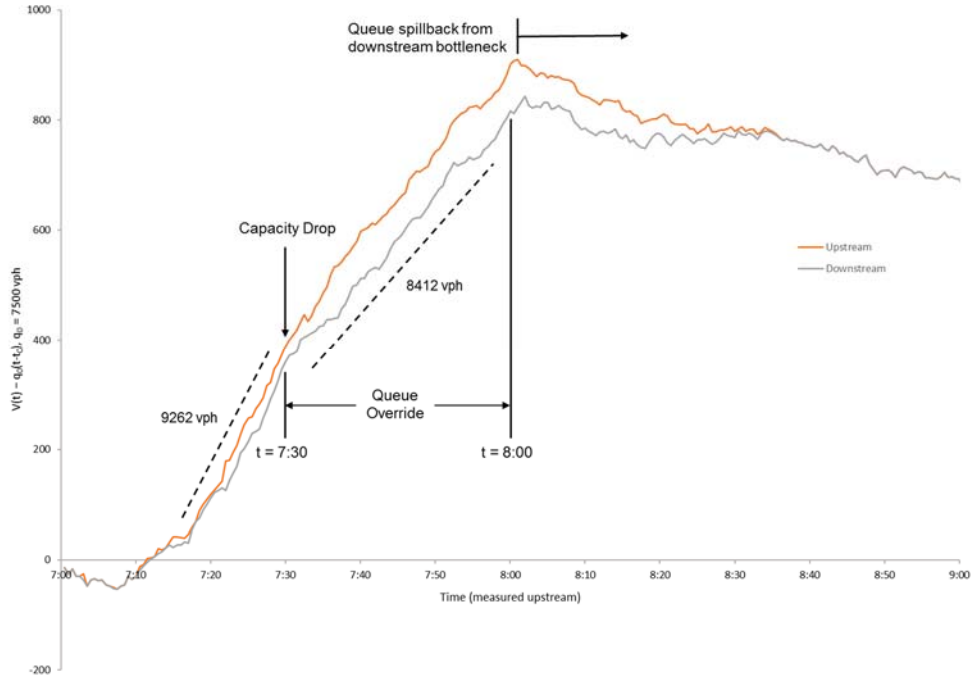
Figure 6.7 Cumulative Vehicle Counts (oblique scale) of May 16, 2016 (Monday)

The $O(t)$ curves shown in Figure 6.8 resemble the similar trends presented in the previous figures. However, due to the presence of multiple incidents during the morning peak period of Tuesday May 17, 2016, data from this day was not used to determine whether queue override causes capacity drop.
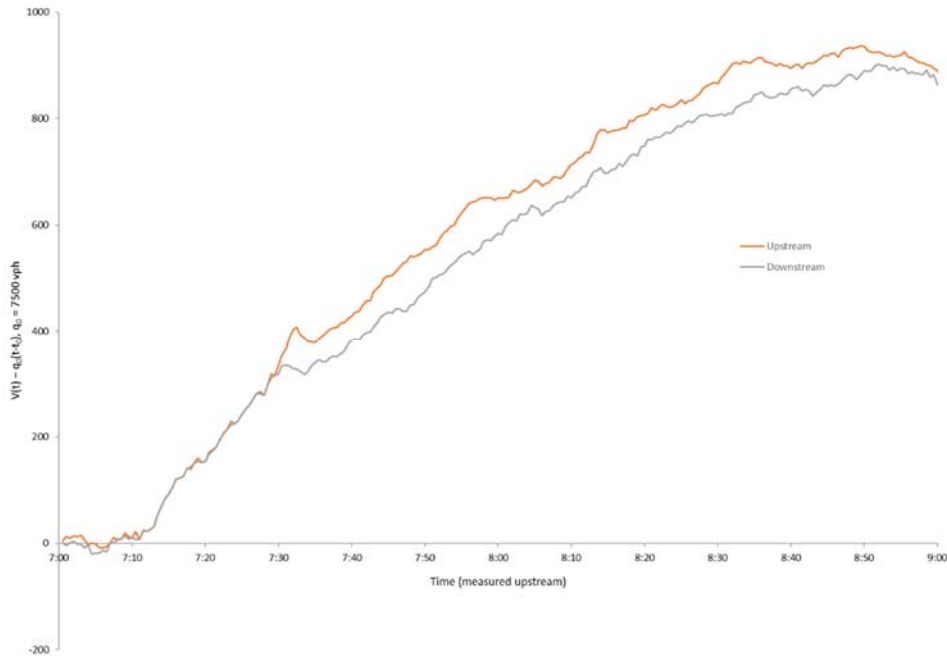
Figure 6.8 Cumulative Vehicle Counts (oblique scale) of May 17, 2016 (Tuesday)

Figure 6.9 shows the cumulative counts obtained from Wednesday May 18, 2016. From the $O(t)$ curves, it can be observed that just before $t = 7:20$ and shortly after, the outflow of the freeway bottleneck remained fairly high in order to accommodate the peak period demand. The $O(t)$ curves overlapped, which indicates that traffic is free-flowing on the freeway mainline and on the section of the on-ramp downstream of the ramp meter. The $O(t)$ curves begins to diverge just before $t = 7:30$ due to the increase in demand, but the high outflow remained roughly the same until $t = 7:35$. As shown by the left hand side dotted line, the observed capacity is 8318 vph.

At $t = 7:35$, there is sufficient on-ramp queue spillback to activate queue override, and queue override was effective up to $t = 8:48$. During the time when queue override remained active, the outflow of the freeway bottleneck reduced to 7870 vph, then to 7813 vph, and eventually to 7368vph, as indicted by the dotted lines. This represents a capacity reduction of 5.39%, 6.07%, and 11.42%, respectively.

The reduction in outflow was not a result of exogenous downstream bottleneck, after verifying that free-flow condition persisted at Berryessa Rd. throughout the morning peak period. In addition to confirming that the bottleneck was isolated, Figure 6.9 shows that the demand did not reduce after queue override activated at $t = 7:35$. Thus, these observations confirmed that queue override resulted in capacity drop.
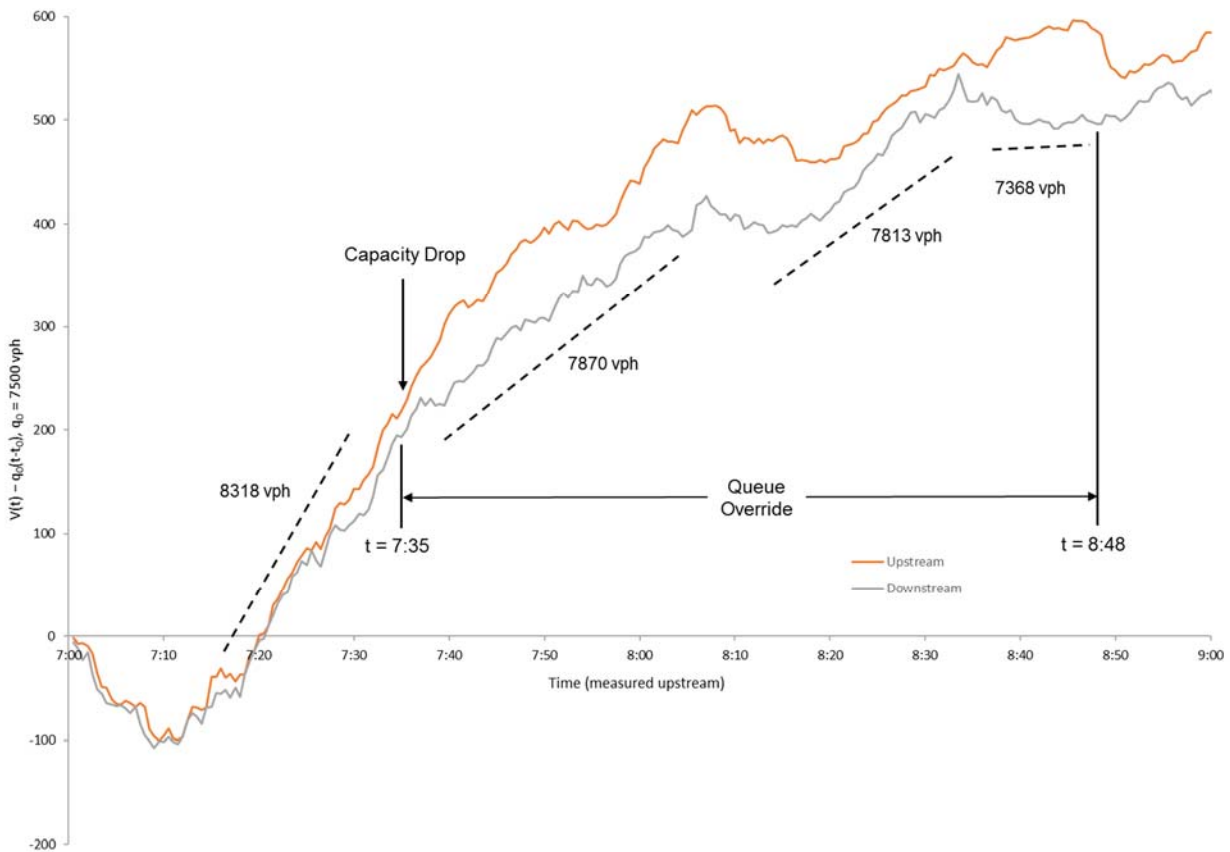
Figure 6.9 Cumulative Vehicle Counts (oblique scale) of May 18, 2016 (Wednesday)

57

Figure 6.10 shows the cumulative counts obtained from Thursday May 19, 2016. Based on the $O(t)$ curves, it can be observed that starting from $t = 7:10$, the outflow of the freeway bottleneck remained fairly high in order to accommodate the peak period demand. The $O(t)$ curves do not overlapped but there is sufficiently high demand to show that the freeway bottleneck is operating at its capacity. The observed capacity is 8749 vph prior to $t = 7:38$, as indicated by the left hand side dotted line.

At $t = 7:38$, there is sufficient on-ramp queue spillback to activate queue override, and queue override was effective up to $t = 8:05$. During the time when queue override remained active, the outflow of the freeway bottleneck reduced to 7918 vph, as shown by the right hand side dotted line. This translates to a 10.5% reduction in capacity.

The reduction in outflow was not a result of exogenous downstream bottleneck, after verifying that free-flow condition persisted at Berryessa Rd. until $t = 8:09$. In addition to confirming that the bottleneck was isolated, Figure 6.5 shows that the demand did not reduce after queue override activated at $t = 7:38$. Data for times beyond $t = 8:09$ were not analyzed due to the fact that the exogenous downstream bottleneck was active from $t = 8:09$ to the end of the morning peak period. Nevertheless, there is sufficient evidence showing that queue override resulted in the observed capacity drop.
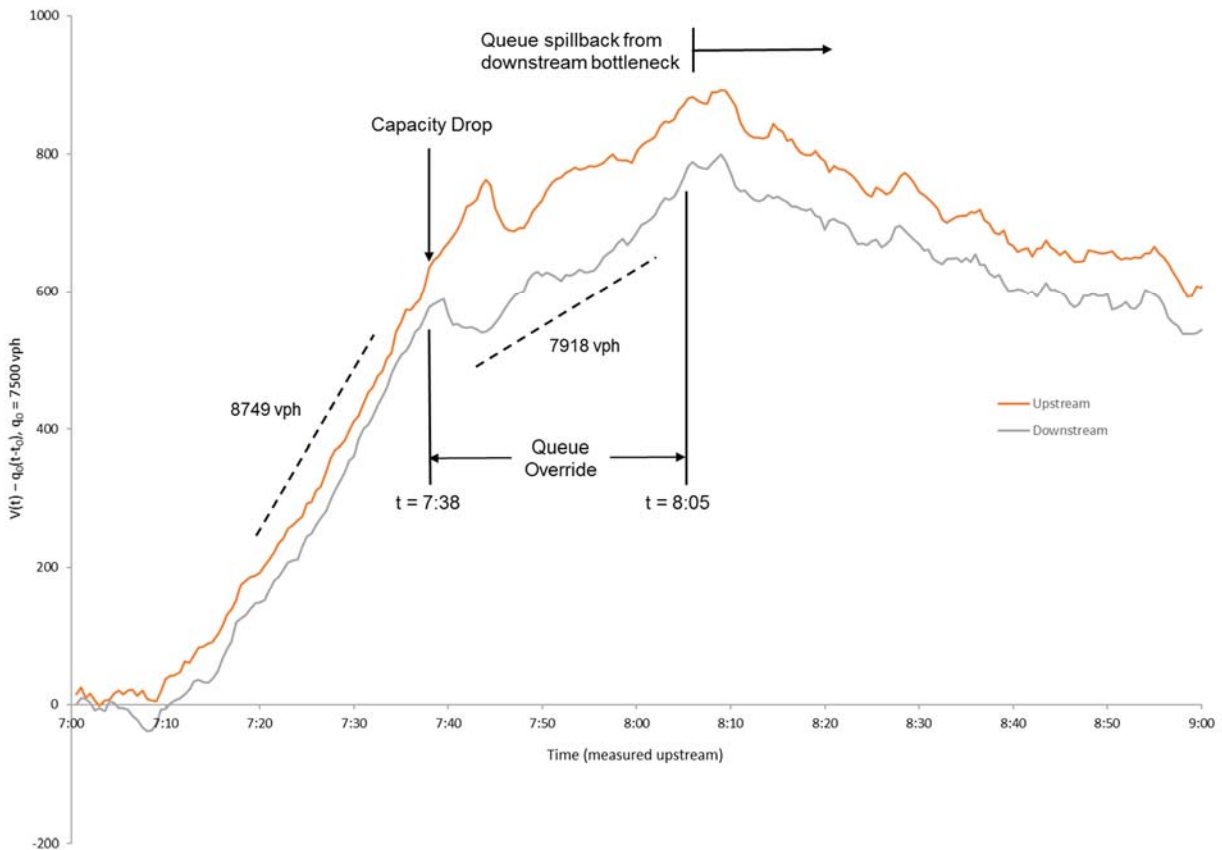
Figure 6.10 Cumulative Vehicle Counts (oblique scale) of May 19, 2016 (Thursday)

Similar to Monday May 9, 2016, the $O(t)$ curves shown in Figure 6.11 reveal that the demand did not exceed the capacity (both curves overlap) on Friday May 20, 2016. However, the outflow between $t = 7{:}30$ and $t = 7{:}50$ is fairly high at 8757 vph. Ramp metering remained active but queue override was not active during the morning peak period, due to insufficient on-ramp demand. Therefore, the existing ramp metering plan maintained the high capacity of the freeway.
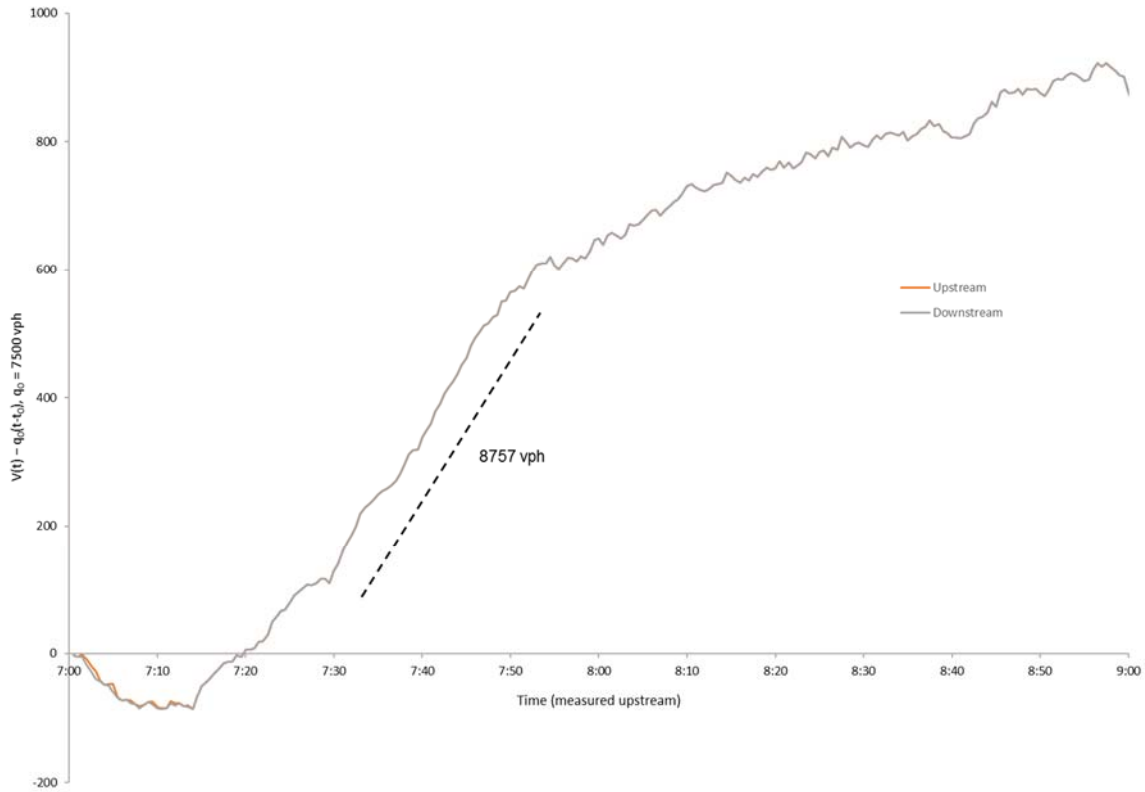
Figure 6.11 Cumulative Vehicle Counts (oblique scale) of May 20, 2016 (Friday)

6.3 Conclusion

The analysis of the field data collected over a two week period suggests that activating queue override reduces the freeway bottleneck capacity by approximately 5% to 10%. This has been confirmed by comparing the freeway bottleneck capacity of the morning peak periods with and without queue override activated. In other words, the results shown suggest that deactivating queue override would increase the freeway capacity and is therefore recommended.

CHAPTER 7

CONCLUSIONS

7.1 Summary of the Study Findings

The objectives of the research project described in this report is to develop and implement a control algorithm to manage the entry of vehicles on the on-ramp through signal timing changes at the intersections along adjacent arterial(s). The report describes the research performed in phase IIA of the project: development of a control algorithm, test site selection, and evaluation of a proposed algorithm on the test site through simulation.

A section of the I-680 Northbound freeway with Capitol Ave. as the parallel arterial in the city of San Jose was selected as the test site. The AM peak was selected as the analysis period. Traffic operations at the site were simulated using the AIMSUN microscopic model. The model was calibrated to reasonably replicate existing traffic operating conditions.

The simulation results show the proposed coordination strategy eliminated the queue spillback on the metered on-ramps that activate the queue override. This resulted in 17.9% reduction on freeway delay. The analysis of field data on bottleneck discharge flows indicate that the proposed strategy may improve the freeway capacity by 5 to 10 percent. The delay on the parallel arterial was increased on the approaches feeding the on-ramps but decreased on the rest of the signal controlled approaches. The system-wide delay was reduced by 7 percent.

The proposed control algorithm (Control Strategy III: queue length minimization) can be used with any freeway on-ramp metering algorithm. The proposed algorithm is simple and readily implementable at most freeway corridors with metered on-ramps and adjacent signalized arterials without additional instrumentation.

7.2 Next Step: Project Phase IIB

The next step in the ongoing research is conducting the Phase IIB of the project: field implementation and testing of the control algorithm at the selected test site. This phase of the project involves the following major tasks: a) strategy software implementation and testing, b) field implementation, c) data collection on traffic performance on both freeway and arterial intersections, and d) analysis of field data to assess algorithm performance and develop guidelines for statewide implementation.

REFERENCES

1. Urbanik, T., D. Humphreys, B. Smith, and S. Levine. Coordinated Freeway and Arterial Operations Handbook. *Federal Highway Administration, Publication No. FHWA-HRT-06-095*, May 2006.

2. Tian, Z., Balke, K., Engelbrecht, R., Rilett, L. Integrated Control Strategies for Surface Street and Freeway Systems. *Transportation Research Record* #1811, TRB, Washington, D.C., 2002, pp. 92-99.

3. Zhang, H., Ma, J., Nie, Y. Local Synchronization Control Scheme for Congested Interchange Areas in Freeway Corridor. *Transportation Research Record* #2128, TRB, Washington, D.C., 2009, pp. 173-183.

4. Zhang, L., Gou, J., Jin, M. Model of Integrated Corridor Traffic Optimization. *Transportation Research Record* #2311, TRB, Washington, D.C., 2012, pp. 179-191.

5. Liu, X., Zhang, G., Kwan, C., Wang, Y., Kemper, B. Simulation-based, Scenario-driven Integrated Corridor Management Strategy Analysis. *Transportation Research Record* #2396, TRB, Washington, D.C., 2013, pp. 38-44

6. Gunther, G., Coeymans, J., Munoz, J., Herrera, J. Mitigating Freeway Off-ramp Congestion: A Surface Street Coordinated Approach. *Transportation Research Part C: Emerging Technologies*, Volume 20, Issue 1, February 2012, pp. 112-124.

7. Yang, X., Cheng, Y., Chang, G. Dynamic Signal Control Strategy to Mitigate Off-ramp Queue Spillback to Freeway Mainline Segment. *Transportation Research Record* #2438, TRB, Washington, D.C., 2014, pp. 1-11.

8. Yang, X., Cheng, Y., Chang, G. Integrating off-ramp Spillback Control with a Decomposed Arterial Signal Optimization Model. *Transportation Research Record* #2487, TRB, Washington, D.C., 2015, pp. 112-121.

9. Tian, Z., Messer, C., Balke, K., Urbanik, T. Integration of Diamond Interchange and Ramp Metering Operations. *Transportation Research Record* #1925, TRB, Washington, D.C., 2005, pp. 100-111.

10. Recker, W., X. Zheng, and L. Chu. *Development of an Adaptive Corridor Traffic Control Model*. California PATH Research Report, Sept. 2009.

11. Li, Z., Tao, R. Integrate Control of Freeway Interchange Model based on Enhanced Cell Transmission Model. *Transportation Research Record* #2259, TRB, Washington, D.C., 2011, pp. 179-191.

12. Su, D., XY. Lu, R. Horowitz, Z. Wang. Coordinated Ramp Metering and Intersection Signal Control, *International Journal of Transportation Science and Technology*, Vol. 3, No. 2, 2014, pp. 179-191.

13. Papageorgious, M., H. Hadj-Salem, and J. Blosseville. ALINEA: A Local Feedback Control Law for On-Ramp Metering.Transportation Research Record# 1320, TRB, Washington, D.C., 1991, pp: 58-64.

14. Lighthill, M. and G. Whitham, On kinematic waves. II. A theory of traffic flow on long crowded roads. *Proceedings of the Royal Society of London. Series A. Mathematical and Physical Sciences*, Vol. 229, No. 1178, 1955, pp. 317-345.

15. Richards, P., Shock waves on the highway. *Operations Research*, Vol. 4, No. 1, 1956, pp. 42-51.

16. Newell, G., *Theory of Highway Traffic Signals*, Institute of Transportation Studies Research Report, UCB-ITS-RR-89-7.

17. Gettman, D., G. Madrigal, S. Allen, T. Boyer, S. Walker, J. Tong, S. Phillips, H. Liu, X. Wu, H. Hu, M. Abbas, Z. Adam, and A. Skabardonis. *Operation of Traffic Signal Systems in Oversaturated Conditions*. National Cooperative Highway Research Program, July 2012.

18. TSS|Aimsun. http://www.aimsun.com/. Accessed on July 29, 2013.

19. Caltrans PeMS. http://pems.dot.ca.gov/. Accessed on July 29, 2013.

20. Dowling, R., A. Skabardonis, and V. Alexiadis, Traffic Analysis Toolbox Volume III: Guidelines for Applying Traffic Microsimulation Modeling Software. *Federal Highway Administration*, *Publication No. FHWA-HRT-04-038*, June 2004.

21. Daganzo, C.F., Fundamentals of Transportation and Traffic Operations. Elsevier, New York.

22. Cassidy, M.J., Windover, J.R., Methodology for Assessing Dynamics of Freeway Traffic Flow. *Transportation Research Record* #1484, TRB, Washington, D.C., 1995, pp. 73-79.

23. Munoz, J.C., Daganzo, C.F., Fingerprinting Traffic from Static Freeway Sensors. *Cooperative Transportation Dynamics* #1, 2002, pp. 1-11.

24. Cassidy, M.J., Rudjanakanoknad, J., Increasing the Capacity of an Isolated Merge by Metering its On-ramp. *Transportation Research Part B* #39, 2005, pp. 896-931.